國立交通大學

電機與控制工程研究所

博 士 論 文

以肌電波為基礎之機器手臂運動控制

Effective Robot Motion Governing Based on Using EMG Signal

研 究 生：劉修任

指導教授：楊谷洋 教授

中 華 民 國 一百 年 一 月

以肌電波為基礎之機器手臂運動控制

Effective Robot Motion Governing Based on Using EMG Signal

研 究 生：劉修任　　Student：Hsiu-Jen Liu

指導教授：楊谷洋　　Advisor：Kuu-Young Young

國 立 交 通 大 學

電 機 與 控 制 工 程 研 究 所

博 士 論 文

A Dissertation

Submitted to Institute of Electrical and Control Engineering

College of Electrical Engineering

National Chiao Tung University

in partial Fulfillment of the Requirements

for the Degree of

Doctor of Philosophy

in

Department of Electrical Engineering

January 2011

Hsinchu, Taiwan, Republic of China

中華民國一百年一月

以肌電波為基礎之機器手臂運動控制

研究生：劉修任　　指導教授：楊谷洋 博士

國立交通大學電機與控制工程研究所博士班

摘要

肌電波（electromyography，EMG)是肌肉收縮過程所產生的生理訊號，含有肌肉收縮之強度與動作之意圖，可作為肢體殘障與年長人士的義肢或機器手臂的控制命令。為建構一套以肌電波為基礎之機器手臂運動操控系統，本論文提出一個簡單又有效率之方法，起始點偵測法 (initial point detection)，其原理為當擷取之特徵(feature)值高於上臨界值時則判定肌肉是處於活動之狀態，直至特徵值低於下臨界值時才判定肌肉停止活動。然個體之模糊性，致使上下臨界值之設定不易，雖由嘗試錯誤法(trial-and-error method)可使分類器達到高的辨識率，但選取過程費工耗時，故引用模糊系統加以改善，其可行性經單自由度(one degree of freedom)機器手臂運動控制獲得確認。然將所提之架構延伸於辨識控制多自由度機器手臂運動之肌電訊號時，發現原方法並不適用於肌肉相互干涉(muscle mutual interference)過大的情況，進而採用希爾伯特-黃轉換法(Hilbert-Huang transform)中之經驗模態分解法(empirical mode decomposition, EMD)，將EMG訊號分解成多個內建模態函數(instrinsic mode function, IMF)，萃取出主要執行運動肌肉之訊號。同時為有效地獲得多個肌肉其上下臨界值合適之歸屬函數，本論文應用適應性類神經模糊推論系統(adaptive neuro-fuzzy inference system, ANFIS)改善傳統模糊系統要由人工調整的缺點。所提之方法既沒有複雜之演算流程，也不須學習與訓練過程，故即時之肌電波機器手臂運動控制得以實現。

Effective Robot Motion Governing Based on Using EMG Signal

Student：Hsiu-Jen Liu Advisor：Dr. Kuu-Young Young

Institute of Electrical and Control Engineering

National Chiao Tung University

Abstract

Electromyography (EMG) signal, as a physiological signal generated during muscle contraction, implicates several important messages, such as the muscular force level and operator's intention. It is very suitable to serve as the control signal for the manipulation of the rehabilitation device, human-assisting robot and others. To develop an effective robot motion governing based on using EMG signal, this dissertation proposes a so-called initial point detection method to discriminate the up limb motion onset by detecting the instant when the magnitude of the extracted EMG feature reaches the upper critical value and offset when that descends to the lower critical value from onset state. Consequently, the mapping between the limb EMG signals and the corresponding robot arm movements can be established very quickly. Meanwhile, due to the individual fuzziness, the tuning of the system parameters for the individual user is not that straightforward. Thus the concept of the fuzzy system is employed so that the tedious process encountered in the trial-and-error method can be avoided. While the proposed system is shown to be effective for robot motion governing, it is not appropriate to serve as a classifier for more than 1-DOF (degree of freedom) limb motion as it has larger muscle mutual interference. To tackle this, the EMD is applied to decompose the EMG signals into several intrinsic mode functions (IMFs). Each IMF represents different physical characteristic, so that the major muscular movements can be recognized. Meanwhile, for multi-DOF limb motion, the fuzzy system adopted for 1-DOF motion is not efficient enough for the tuning of the critical values for each individual user. For its excellence on adaptation, the adaptive neuro-fuzzy inference system (ANFIS) is employed to realize the fuzzy system. Because neither complicated computation nor training and learning processes are needed, the proposed scheme not only simplifies system complexity, but also increases the efficiency in motion governing.

Acknowledgements

感謝國家太空中心提供在職進修的機會及中心長官、同仁給予的支持與鼓勵，讓我一圓擁有博士學位的夢想。更要感謝指導教授楊谷洋博士在攻讀學位期間的指導與支持。老師的諄諄教誨，使我獲益良多。

亦感謝宋開泰教授、羅佩禎教授、周志成教授、楊秉祥教授、蘇木春教授、蔡清池教授與李慶鴻教授於口試時給予的寶貴意見，使本論文得以更臻完美，謹此致上最誠摯之謝意。

在眾多親朋好友的協助下，本論文得以順利完成。感謝同事文雄、竣吉，同學木政、豪宇、怡康、明勳、柏穎，兄姐玉琴、修程、玉彥、修安，大嫂美香及娌姪詠慧、哲維、哲宇在實驗上的鼎力相助，才有豐碩的成果可以呈獻。感謝鶴年兄與浩基兄在期刊論文的校對，還有「人與機器實驗室」的同窗，由於你們論文研讀心得的分享，才激發出我的研究靈感與思維，在此亦表感謝。

求學生涯雖正式畫下句點，但不代表學習就此結束。今後將秉持著師長的教誨與活到老學到老的精神，繼續充實自己，並奉獻自己的專業所學於職場上，以不負師長的期望與中心的栽培。

最後謹以此論文獻給養育我的母親、天上的父親及愛護我的親朋好友們。

Contents

List of Tables

List of Figures

Chapter 1

Introduction

Nowadays, the number of disabled and elderly is increasing. With a decreasing birthrate, the development of the human-assisting manipulators is imperative for them to alleviate the dependence and improve the quality of life. Teach box, joystick, and keyboard, are traditional devices used for manipulation. Currently, voice control also becomes an alternate [1]. Along with the development in the areas of sensing and measurement techniques, signal processing, and biomedical engineering, it is no longer a dream by using the physiological signals to serve as the control signal for the computer, home appliances, mechanical devices, etc.

EMG is a physiological signal generated from the exchange of ions across muscle fiber membranes during muscle contraction. Its amplitude ranges between 0~10 mV (peak to peak) or 0~1.5 mV (root mean square). Its frequency, varying according to the motion and individual, ranges between 0~500 Hz, with a distribution mainly around 50~150 Hz [2]. By applying the conductive elements or electrodes on the skin surface, or invasively within the muscle, EMG signal can thus be measured. As EMG implicates several important messages, such as the muscular force level and operator's intention, it is very suitable to serve as the control signal, and also leads to a natural and intuitive manipulation. Researchers have devoted to the study of applying EMG for controlling human-assisting robots and

rehabilitation devices for the physically handicapped as well as the elderly to improve their life quality. Fukuda et al. [3] proposed teleoperating a human-assisting manipulator by using EMG signals. Artemiadis and Kyriakopoulos [4] proposed an EMG-based position and force control scheme for robot arm. Ferreira et al. [5] applied the EMG and EEG (electroencephalogram) for developing the interfaces for robot systems. Gao et al. [6] developed a robotic arm wrestling system based on EMG and artificial neural network. Gopura and Kiguchi [7] developed exoskeleton robots for assisting the motion of physically weak individuals based on EMG and fuzzy control. Ito et al. [8] presented prosthetic speed control by utilizing the relation of the proportion of muscular contraction level. Oppenheim et al. [9] proposed using EMG as an input device for the Nintendo Wii™ video game console. Huang et al. [10] proposed using the EMG signals combined with the pattern recognition technique to identify user locomotion modes. Aso et al. [11] presented using EMG to drive the electric car. And, Harada et al. [12] proposed using EMG to control robot finger.

Because EMG exhibits high nonlinearity and fuzziness [13-15], even for the same motion executed by the same person, different EMG measurements may be obtained under different circumstances. Among these researches, EMG signals were identified to be affected by noises, such as ECG (electrocardiogram) crosstalk, electromagnetic induction from power lines, and arm and cable movements. Meanwhile, muscle mutual interference, physiological condition (e.g., fatigue), skin impedance and temperature, etc., also contribute to the fuzziness of the

EMG signals, which are time-varying and highly nonlinear. These properties result in the difficulty in extracting proper EMG features for motion classification.

To extract and recognize the intended movement pattern from EMG, several methods have been proposed, in time domain, such as mean absolute value, variance, bias zero-crossing, Willison amplitude, autoregressive model [16-18], Euclidean distance and standard deviation [19], and hidden Markov model [20] , etc., and in frequency domain, such as Fourier transform [21] and wavelet analysis [22, 23]. However, those approaches in the time domain induce high computational complexity [17]. Meanwhile, EMG signals are nonlinear and non-stationary signals, especially for contraction levels higher than 50% of maximum voluntary contraction (MVC) [24]. But the data must be linear and strictly stationary for Fourier transform [25]. As for the wavelet analysis, a mother wavelet has to be defined a priori [26]. Unsuitable mother wavelet may lead to unsatisfactory results. Some researchers proposed using the learning approach, e.g., the neural network [6, 27, 28], and reported salient performance. But, the learning approach demands certain computational load and incurs some system complexity for the learning and training processes involved.

Alternatively, Hilbert-Huang transform (HHT) is a time-frequency method. Based on the local time scale of the data, it decomposes a signal into several intrinsic mode functions (IMFs) via empirical mode decomposition (EMD), and then calculates the instantaneous frequency of each IMF at any point in time via Hilbert transform. Hence, it can be used for

nonlinear and non-stationary data analysis. HHT has been broadly applied in numerous scientific disciplines and investigations, e.g., analysis on the bioelectricity signal, failure testing, and earthquake signal etc. [29]. Several researchers have applied HHT to EMG related studies. Xie and Wang. [24] and Peng et al. [30] adopted HHT to find the features of muscular fatigue. Ma and Luo [29] proposed using HHT and AR-model to extract the sEMG feature to recognize the hand-motions. Wang et al. [31] presented a feature extraction technique based on empirical mode decomposition to classify the walking activities from accelerometry data. Chen et al. [32] employed HHT to extract the frequency features of the stump to control transfemoral prosthesis. Zong and Chetouani [25] presented a feature extraction technique based on HHT for emotion recognition from physiological signals.

1.1 Motivation

To develop an EMG based human-assisting manipulator needs to well consider the influence from the muscle type, strength of muscle contraction, fatigue level, strategy in performing the task, and others. Several EMG based human-assisting manipulators have been proposed, whose feature extraction and classification/recognition designs are summarized in Table 1-1. These manipulators require either complicated computation or tedious training and learning processes, as a result, the practicality is decreased. As the commercial prosthesis have no profound theory and complex mechanism, meanwhile, their operations are simple and easy,

we, therefore, propose a simple and effective system for governing robot arm motion via the upper limb EMG signal, whose feature extraction and classification designs are listed in Table 1-1 as well. With the assistance of the proposed system, the physically weak individual (disabled, injured or elderly) can do some important daily activities such as eating from spoon, drinking from cup and pouring from a bottle, etc. by themselves without needing assistance from others. In addition to the robot arm motion governing, the proposed method can further be used for governing the different fundamental applications, such as the devices with bidirectional commands (on/off, increment/decrement), prosthetic hand, TV and radio for instance.

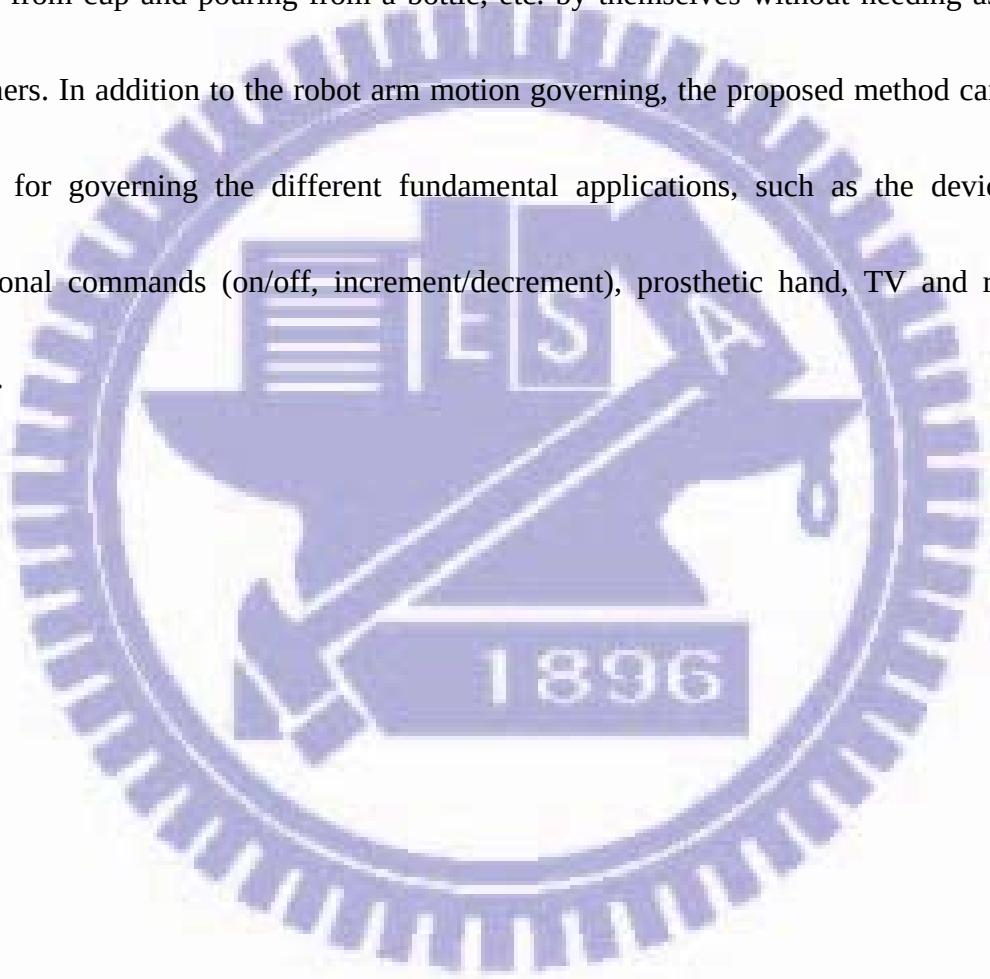

Table 1-1 EMG based human-assisting manipulators

Human-assisting manipulators	EMG Channel	Feature Extraction	Classification/ Recognition	Reference
Robot finger	3	Fast Fourier transform	Neural network	[12]
Robot exoskeleton	8	MAV	Neuro-fuzzy approach	[14]
Prosthetic hand	2	VAR, BZC, autoregressive model, and spectral estimation	Artificial neural network	[17]
Transfemoral prosthesis	5	Hilbert-Huang transform		[32]
Robot arm	11	Integral of absolute value, zero corssing, VAR, Median frequency	Switching regime decoding model, principal component analysis,	[33]
Robot arm	4	Initial point detection	EMD	This dissertation

1.2 Contribution

The contribution of this dissertation is proposing an EMG-base robot control system to provide a natural and intuitive manipulation for governing robot arm motion. The presented initial point detection method [34, 35] discriminates the upper limb motion onset by detecting the instant when the magnitude of the extracted EMG feature reaches the upper critical value (CV_u) and offset when that descends to the lower critical value (CV_l) from onset state.

Consequently, the mapping between the upper limb EMG signals and the corresponding robot arm movements can be established very quickly. Meanwhile, due to the individual fuzziness, such as the muscular fatigue, skin impedance and temperature, and muscle mutual interference, etc., the tuning of the system parameters for the individual user is not that straightforward. As an effective means for tackling the system with uncertainties [36-38], thus the concept of the fuzzy system is employed, so that the tedious process encountered in the trial-and-error method can be avoided. Because neither complicated computation nor training and learning processes are needed, this method not only simplifies system complexity, but also increases the efficiency in motion governing. While the proposed system is shown to be effective for robot motion governing, it is not appropriate to serve as a classifier for more than 1-DOF (degree of freedom) limb motion, as limb motion of multi-DOF induces larger muscle mutual interference. To tackle this, the EMD is applied to decompose the EMG signals into several IMFs. Each IMF represents different physical characteristic, so that the major muscular movements can be recognized. To reduce the computational load in EMD, a sixth-order band-pass Butterworth filter and a dedicated data sampling window are employed. Meanwhile, for multi-DOF upper limb motion, the fuzzy system adopted for 1-DOF motion is not efficient enough for the tuning of the CV_u and CV_l for each individual user. For its excellence on adaptation, the adaptive neuro-fuzzy inference system (ANFIS) [39-42] is employed to realize the fuzzy system. The ANFIS has been successfully implemented in

biomedical engineering for classification [43-46] and robot control [47, 48]. A series of experiments are performed to demonstrate the effectiveness and feasibility of the proposed system in governing a 3-DOF robot arm motion via four surface EMG electrodes placed on Biceps Brachii, Triceps Brachii, Pectoralis Major, and Teres Minor. While the results are shown to be effective for robot motion governing, the limitation of this system is that fixed critical values (*CVs*) are suitable for robot motion governing for about 5 ~ 10 minutes, depending on the complexity of the motion. After that, the fatigue of the muscle led to inconsistent classification. We suggest the proposed system not to be used when the subject feels fatigued. Meanwhile, at this stage of the research, this EMG-based robot control system will be based on human upper-limb motion, as a starting point.

1.3 Organization

In Chapter 2, the proposed EMG-based upper-limb robot control system is described, including the modules for EMG signal measurement and processing, feature extraction, and motion classification. Chapter 3 describes the experimental setup, design and experimental results for 1-DOF robot arm movement control. Those for 3-DOF robot arm movement are presented in Chapter 4. Finally, conclusions along with some future works are given in Chapter 5.

Chapter 2

Proposed EMG-Based Upper-Limb Robot Control System

To provide a simple and effective approach for governing robot arm motion in real time via EMG signals, we propose using upper limb EMG signals to develop an EMG-based robot motion governing system as the movements involved in it are not complicated. Figure 2-1 shows the system diagram of the proposed EMG-based upper-limb robot control system, which consists of three main modules: signal measurement and processing, feature extraction, and motion classification. The signal measurement and processing module measures the raw EMG signals of the upper limb and also filters out the noises. The filtered EMG signals are then sent to the feature extraction module to derive their features. With these features, the motion classification module determines the corresponding arm movements and generates the commands to drive the human-assisting robot. From the resultant robot motion, the operator evaluates the performance and determines the next movement. These three modules are described below.

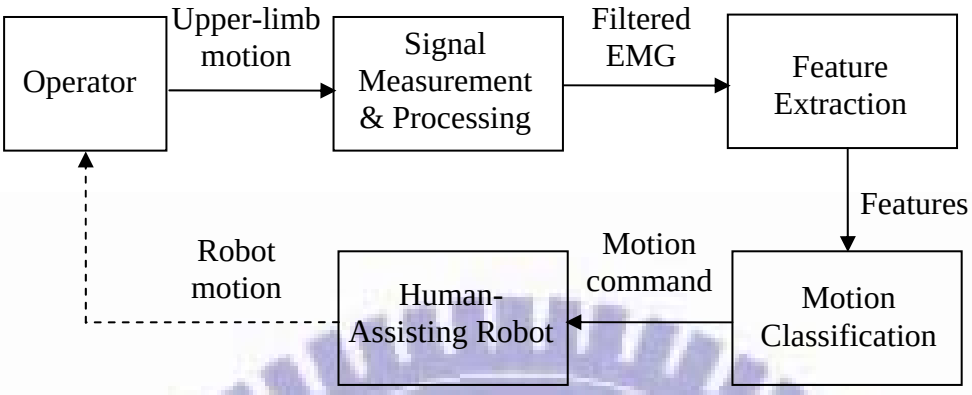

Figure 2-1 Proposed EMG-based upper-limb robot control system

2.1 Signal Measurement and Processing

For EMG signal measurement, the locations and areas of those muscles involved during upper limb movement are needed to consider. The measurement also depends on the regions where the electrodes are placed. To obtain more precise EMG signals, the electrodes need to be placed on the midline of the muscle belly, with the electrodes aligned parallel to the muscle fibers. The recommended inter-electrode distance (from one differential electrode to the other) is about 1~2 cm [2, 49]. Several types of noises may affect the measurement of the EMG signals, such as ECG crosstalk, electromagnetic induction from power lines, and arm and cable movements. The ECG crosstalk can be suppressed by measuring signals from those

muscles away from the heart. The frequency of the electromagnetic noise is around 60 Hz. While a notch filter at that frequency can be an option, it should be avoided, because EMG has large signal contributions at these and neighboring frequencies. We thus let the proposed approach tackle its influence as the disturbance. Meanwhile, the frequency distribution for the arm and cable movements is around 0 to 20 Hz, which can be tackled using a high-pass filter.

2.2 Feature Extraction

To extract and recognize the intended movement pattern from EMG, several methods have been proposed, in time domain, such as mean absolute value (MAV), variance (VAR), bias zero-crossing (BZC), Willison amplitude (WAMP) [16,17], autoregressive model, Euclidean distance and standard deviation, and hidden Markov model , etc., and in frequency domain, such as Fourier transform and wavelet analysis. Among them, MAV, VAR, BZC and WAMP are four famous feature extraction indices for EMG signal. The formulae for these indices are listed in Table 2-1, in which X_k denotes the *k*th sampling data in the window for computing the feature and *N* is the window length. MAV is taken as the estimation for signal power and VAR that for power density. Both MAV and VAR are frequently used to estimate the contraction level of the muscle. BZC, which includes a bias value for dealing with noise

interference, counts the zero-crossing, i.e., the number of times the signal passes the zero value. And, WAMP is used to count the number of times the signal amplitude exceeds a predefined threshold, indicating the contraction level of the muscle. The proposed system adopts MAV as the feature extraction index, because we intend to evaluate the contraction level of the muscle. Meanwhile, VAR can also be an alternative.

Table 2-1 Feature extraction name and formula

Name	Formula
MAV	$MAV = \frac{1}{N}\sum_{k=1}^{N}\lvert X_k \rvert$
VAR	$VAR = \frac{1}{N-1}\sum_{k=1}^{N} X_k^{\,2}$
BZC	$BZC = \sum_{k=1}^{N}\mathrm{sgn}\left[(X_k - 0.4)\times(X_{k-1} - 0.4)\right]$ $\mathrm{sgn}(x) = \begin{cases} 1\ , \text{ if } x > 0 \\ 0\ , \text{ others} \end{cases}$
WAMP	$WAMP = \sum_{k=1}^{N} f(\lvert X_k - X_{k-1} \rvert);$ $f(x) = \begin{cases} 1\ , \text{if } x > threshold \\ 0\ , \text{if otherwise} \end{cases}$

However, the aforementioned methods are not appropriate to serve as a classifier for more than one-DOF upper limb motion as it has larger muscle mutual interference. Alternatively, the EMD method is one of solutions as it decomposes the EMG signals into several IMFs. Each IMF represents different physical characteristic and strength, so that the major muscular movement can be recognized. The following is an introduction of the EMD process.

Figure 2-2 shows the flow chart of the EMD process, which deconstructs the complete signal into a set of IMFs in eight steps (with Steps 1 to 5 for the sifting process) [32, 50]:

Step 1: Identify the local maxima in the filtered EMG data $x(t)$ by interpolating between the maxima and connect them via a cubic spline curve to obtain the upper envelope $U(t)$.

Step 2: Apply the same actions in Step 1 to identify the local minima and obtain the lower envelope $L(t)$.

Step 3: Compute the mean value of the upper and lower envelope $m_1(t)$:

$$m_1(t) = \frac{U(t) - L(t)}{2} \tag{2-1}$$

Step 4: Subtract the running mean value $m_1(t)$ from the original data $x(t)$ to obtain the first component $h_1(t)$:

$$h_1(t) = x(t) - m_1(t) \tag{2-2}$$

Step 5: Iterate Steps 1-4 on $h_1(t)$ for k times until the resulting component $h_{1k}(t)$ ($h_{1(k-1)}(t) - m_{1k}(t)$) satisfies two conditions: (a) the difference between the number of local extremes and that of zero-crossings is zero or one and (b) the running mean value is zero.

Step 6: Designate $c_1(t) = h_{1k}(t)$ if h_{1k} meets the two requirements mentioned above.

Step 7: Subtract the first IMF $c_1(t)$ from the original data to obtain the residual $r_1(t)$:

$$r_1(t) = x(t) - c_1(t) \tag{2-3}$$

Step 8: Treat $r_1(t)$ as the new data and repeat Steps 1-7 on $r_1(t)$ to obtain all the subsequent i.e., $r_2(t)=r_1(t)-c_2(t)$,…, $r_n(t)=r_{n-1}(t)-c_n(t)$ until the final residual $r_n(t)$ meets the predefined stopping criteria as a monotonic function, considered as the trend.

Based on the procedure above, the original data $x(t)$ can be exactly reconstructed by a linear superposition:

$$x(t)=\sum_{i=1}^{n} c_i(t)+r_n(t) \tag{2-4}$$

where n is the number of IMFs.

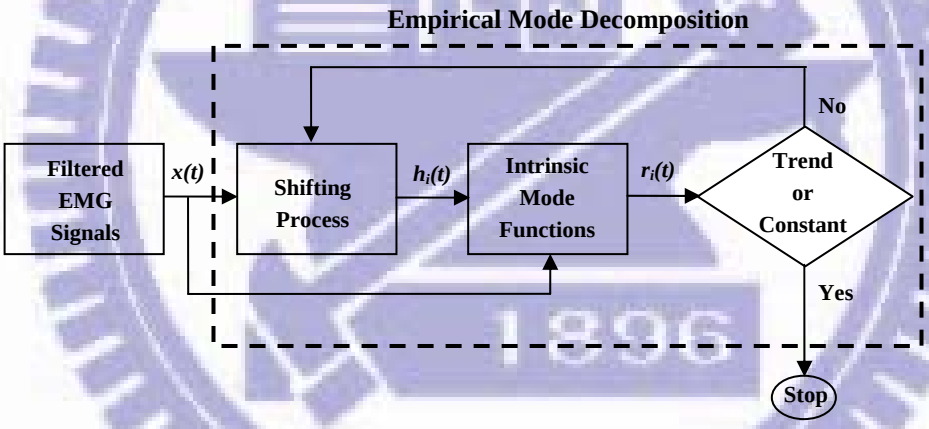

Figure 2-2 Flow chart for empirical mode decomposition

The number of IMFs depends on the characteristic of data. A complex data can be decomposed into more IMFs, which increases the computational load in EMD. As EMG signals are complex physiological signals, high data sampling window results in the fact that the mapping between the upper limb EMG signals and the corresponding robot arm

movements can not be established in the expected time. After several experiments, we found combining a sixth-order band-pass Butterworth filter with a window with 20 samples per second can reduce the computational load, meanwhile, the sampled data can be decomposed into three IMFs within one second. Among which, the 2nd IMF is on behalf of the limb movement. Figure 2-3 shows an example of the EMD process on the dedicated EMG data sampling window when muscle relaxes and flexes. Each of them includes the empirical EMG signal x(t), three IMFs ($c_1(t)$, $c_2(t)$, $c_3(t)$), and residue ($r_3(t)$). The summation of IMFs and residue exactly equals to the empirical EMG signal. By judging from Figures 2-3(a) and (b), $c_1(t)$ shall be the background noise induced by skin impedance and temperature, cable movement, etc., since its magnitude does not vary with arm movement evidently. In contrast, those of $c_2(t)$ and $c_3(t)$ are varied. As the strength of the magnitude of $c_2(t)$ increases when muscle flexes, therefore, $c_2(t)$ is on behalf of the limb movement.

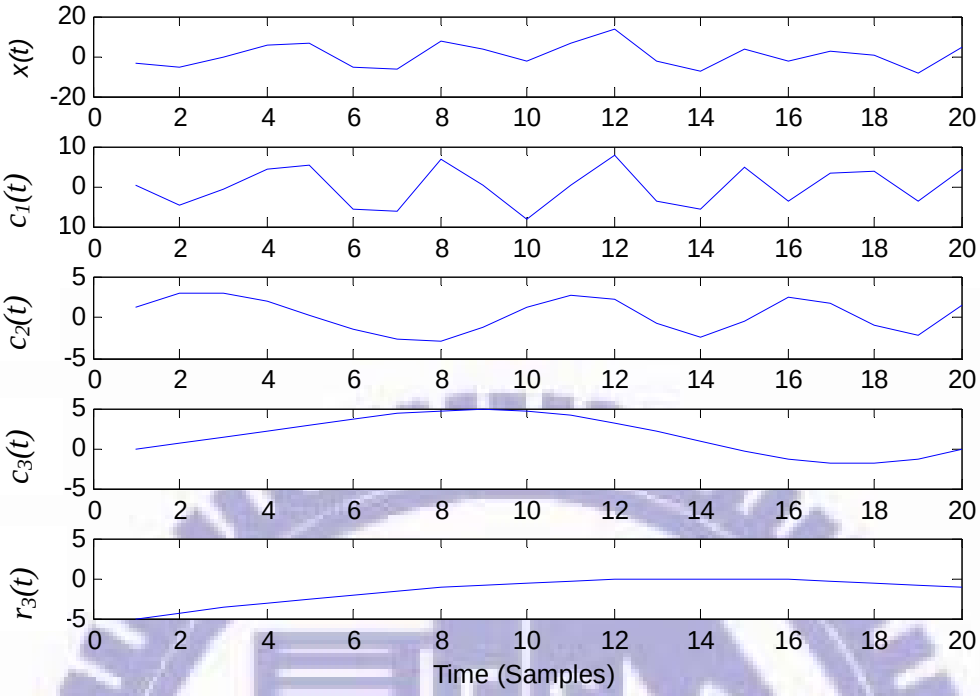

(a) Muscle in relaxation

Figure 2-3 An example of empirical EMG signal and corresponding empirical mode decomposition components, including 3 IMFs and 1 residue (trend): (a) muscle in relaxation and (b) muscle in flexion.

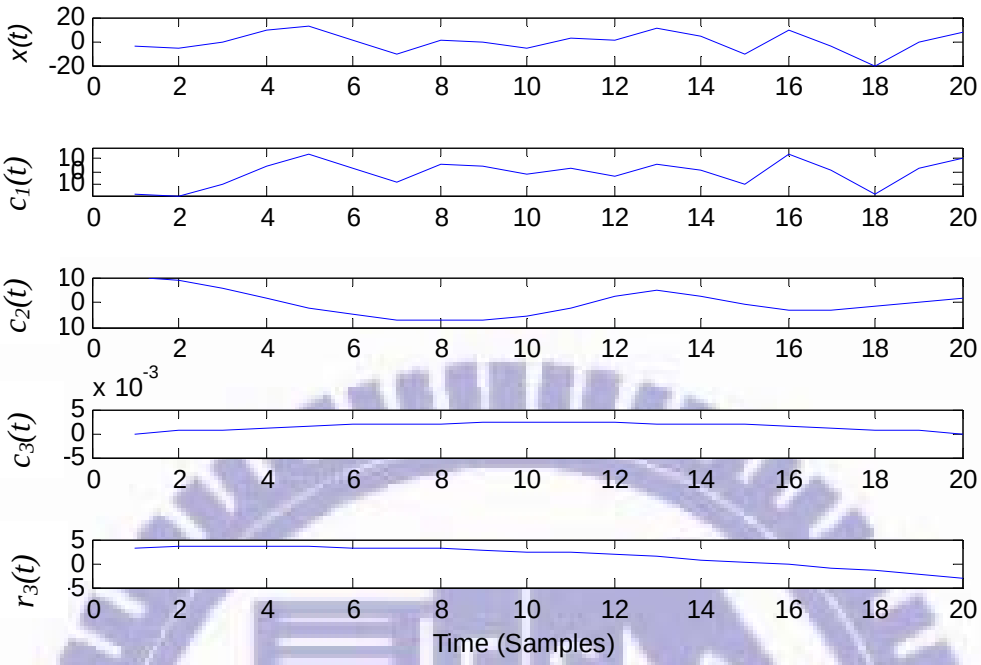

(b) Muscle in flexion

Figure 2-3 (Cont.) An example of empirical EMG signal and corresponding empirical mode decomposition components, including 3 IMFs and 1 residue (trend): (a) muscle in relaxation and (b) muscle in flexion.

2.3 Motion Classification

2.3.1 Initial Point Detection

Because the movements involved in the proposed system are not complicated, an initial point detection method is proposed to deduce the motion intention from the EMG signal. The

reason for the naming is because this method determines the onset of the upper limb motion via detecting the instant when the magnitude of the extracted EMG feature reaches the critical values. Due to its simplicity, real-time motion governing can be achieved. In the proposed classifier design, we start with the single critical value detection, in which the state of the muscle *MS* is determined by checking if the initial value for the feature exceeds a predefined critical value:

$$MS = \begin{cases} 1, & if \quad F_k > CV \\ 0, & otherwise \end{cases} \tag{2-5}$$

where F_k stands for the k th feature and *CV* the critical value. An active *MS* corresponds to an ``ON'' robot command and an inactive one for that of ``OFF'', as illustrated in Figure 2-4(a). Figure 2-5 shows an example, in which MAV is used to evaluate the EMG signal of Biceps Brachii. In Figure 2-5, section A indicates the muscle state during relaxation, and section B that during flexion, both of which exhibit some fluctuations. We thus propose a concept of double critical value detection, as illustrated in Figure 2-4(b). In Figure 2-4(b), the state of the muscle *MS* is determined to be active when the initial value for the feature F_k is larger than the upper critical value CV_u, and *MS* inactive when F_k is smaller than the lower critical value CV_l:

$$MS = \begin{cases} 1, \ if \ \ F_k > CV_u \\ 0, \ if \ \ F_k < CV_l \end{cases} \tag{2-6}$$

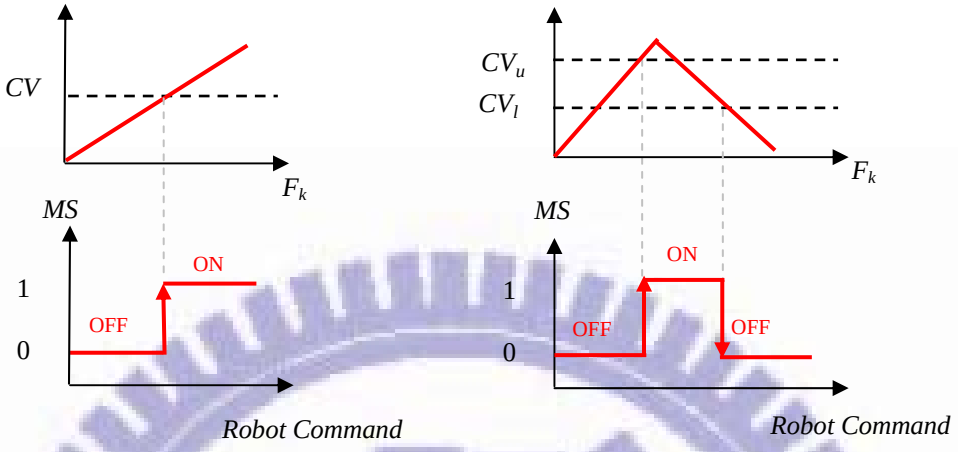

(a) Single critical value (b) Double critical value

Figure 2-4 Conceptual diagram for single and double critical value detection: (a) single critical value and (b) double critical value.

The selection of CV_u and CV_l depends on the following observations. A large CV_u implies that the user has to generate a large force to move the robot arm. It may lead to muscle fatigue, in addition to the increase of the crosstalk between muscles. Contrarily, a small CV_u results in low tolerance against the noise. Meanwhile, a large CV_l may make the robot arm stop its movement earlier than that of the user, while a small CV_l leads to the opposite. The approaches of the trial-and-error method and fuzzy system can be utilized for determining CV_u and CV_l.

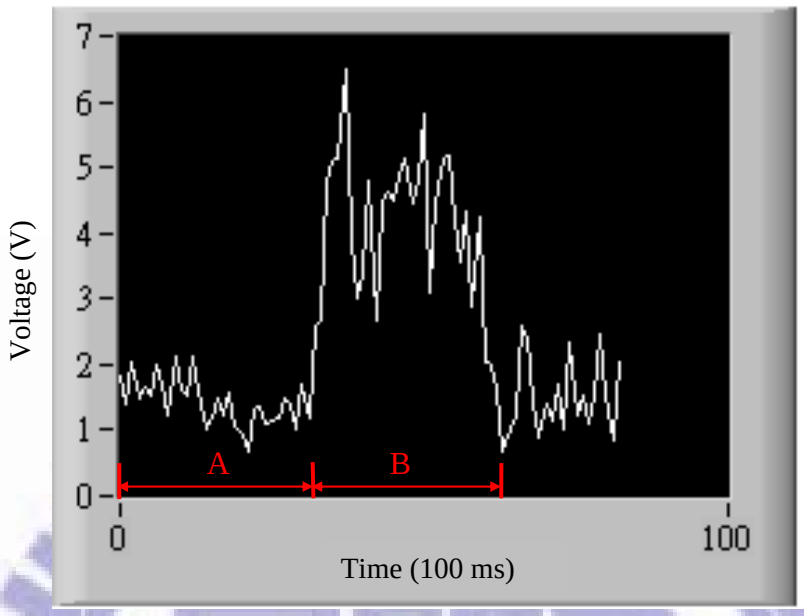

Figure 2-5 An example of EMG signal evaluation of Biceps Brachi using MAV.

To demonstrate that *CVs*, CV_u and CV_l, can be set to be fixed under certain condition in a period of time, we chose a set of fixed *CVs* empirically and performed the motion of elbow up and down for fifty times continuously. The experimental results in Figure 2-6 show consistent classification, except the twenty-fifth trial (marked in red). The entire process lasted for about 10 minutes. After that, the fatigue of the muscle led to inconsistent classification. It indicates that fixed *CVs* are appropriate for the proposed system to govern robot motion for a certain period of time, but should not be used when the subject felt fatigued.

Several factors influence the realization of the classifier, including feature selection, number of samples for feature extraction, and choice of the *CVs*. It is suggested to use

features with smooth waveforms. A larger number of samples may be helpful for feature extraction, at the expense of efficiency and delay.

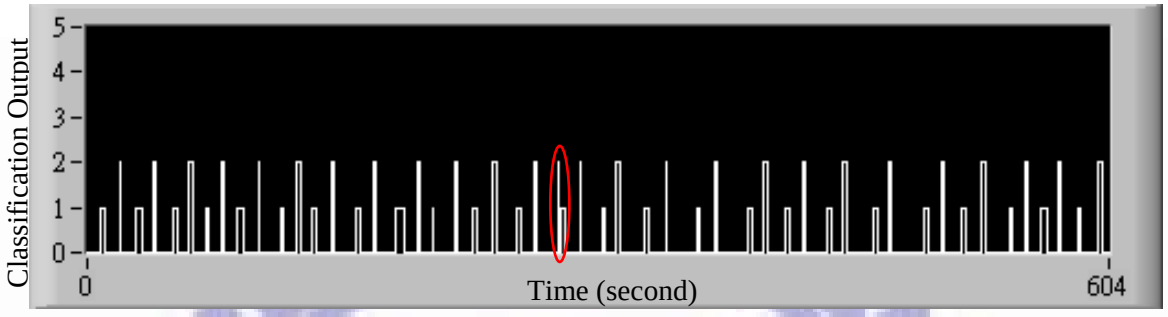

Figure 2-6 Feasibility evaluation by performing the motion of elbow up and down for fifty times continuously (numbers 0-3 correspond to STOP, UP, DOWN, and ERROR, respectively).

Chapter 3

Experimental Design

The proposed EMG-based upper-limb robot control system is using four sets of electrodes placed on Biceps Brachii (BB), Triceps Brachii (TB), Pectoralis Major (PM), and Teres Minor (TM), as shown in Figure 3-1, to control the robot arm movement of either one DOF or multi-DOFs. For the proposed detection method, the classifier is designed to let the feature extracted from the BB correspond to upper limb flexion, that from the TB for extension, that from PM for internal rotation, that from TM for external rotation, that from the synthesis of BB and PM, for flexion-internal rotation, and that from the synthesis of TB and TM for extension-external rotation. Their muscle states will determine whether it is an up, down, turn-left, turn-right, up-left and down-right movement. Due to some muscle crosstalk or imprecise feature identification, sometimes it may lead to conflict movement decision between the two muscles. Under such circumstances, the classifier will output an error signal. Therefore, there are eight outputs for the classifier: STOP, UP, DOWN, LEFT, RIGHT, UP-LEFT, DOWN-RIGHT and ERROR.

Table 3-1 summarizes the mapping from EMG to robot movement. When EMG signals from all channels (CH1~4) are determined to be OFF, the classifier outputs 0 as relaxation; ON for CH1 and OFF for the others, outputs 1 as flexion; ON for CH2 and OFF for the others, outputs 2 as extension; ON for CH3 and OFF for the others, outputs 3 as internal rotation; ON

for CH4 and OFF for the others, outputs 4 as external rotation; simultaneously ON for CH1 & CH3 and OFF for the others, outputs 5 as flexion plus internal rotation; simultaneously ON for CH2 & CH4 and OFF for the others, outputs 6 as extension plus external rotation; and simultaneously ON for undefined channels, outputs 7 as error detection. Figure 3-2 illustrates the classification outputs corresponding to the robot arm movements.

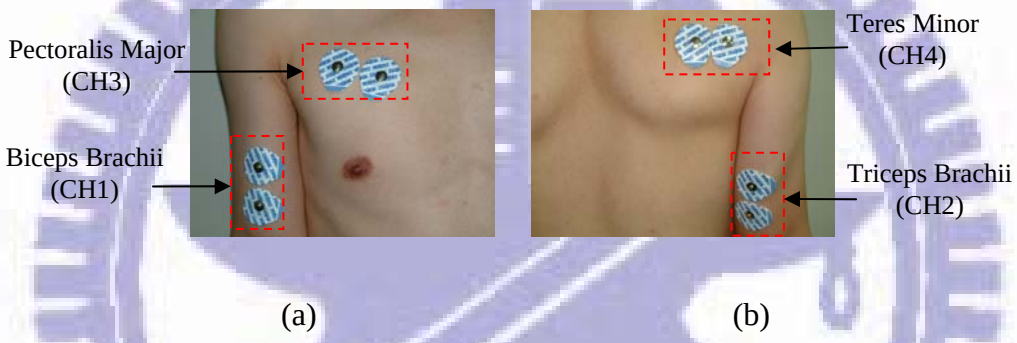

Figure 3-1 Electrode locations: (a) Biceps Brachii and Pectoralis Major, and (b) Triceps Brachii and Teres Minor.

Table 3-1 Mapping from EMG to robot movement

EMG				Upper Limb Status	Classifier Output	Robot Arm
BB (CH1)	TB (CH2)	PM (CH3)	TM (CH4)			
OFF	OFF	OFF	OFF	Relaxation	0	STOP
ON	OFF	OFF	OFF	Flexion	1	J2 axis UP
OFF	**ON**	OFF	OFF	Extension	2	J2 axis DOWN
OFF	OFF	**ON**	OFF	Internal Rotation	3	J1 axis TURN LEFT
OFF	OFF	OFF	**ON**	External Rotation	4	J1 axis TURN RIGHT
ON	OFF	**ON**	OFF	Flexion-Internal Rotation	5	J5 axis UP
OFF	**ON**	OFF	**ON**	Extension-External Rotation	6	J5 axis DOWN
The others				Error	7	STOP

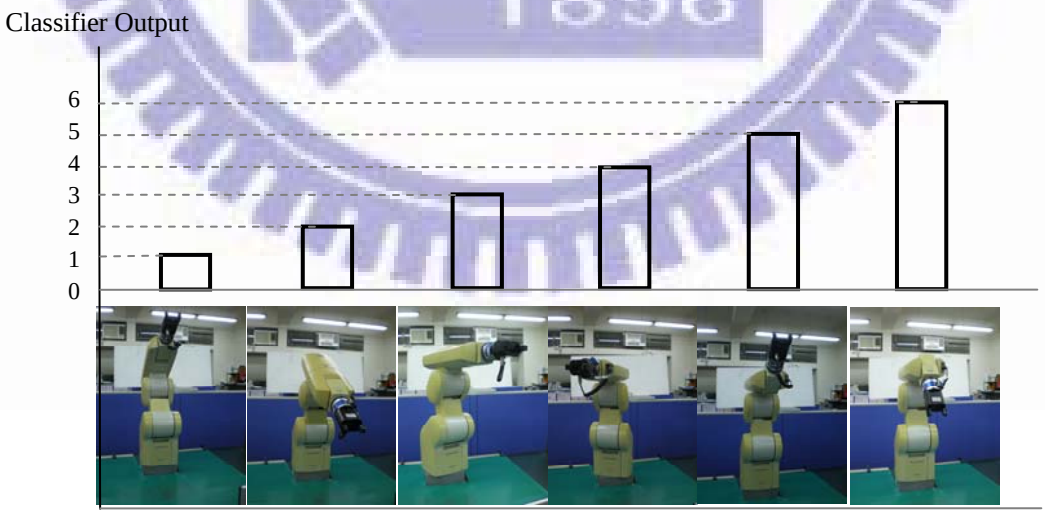

Figure 3-2 Illustrations of classification outputs corresponding to the robot arm movements

3.1 Experimental Setup

A series of experiments were performed to evaluate the performance of the proposed system. Figure 3-3 shows the implementation of the proposed system for experiments. In Figure 3-3, the measured EMG signals are first amplified using the ETH-256 physiological signal amplifier (manufactured by iWorx Systems, USA, the specifications are listed in Table 3-2 and the hardware is shown in Figure 3-4), and the amplified analog signals (voltages) then transformed into digital signals via National Instrument USB-6009 A/D data acquisition device (the specifications are listed in Table 3-3 and the hardware is shown in Figure 3-5) with 1KS/s sampling rate. The digital signals are further forwarded to the LabVIEW development system, as Figure 3-6 shown, which includes a sixth-order band-pass Butterworth filter with the cut-off frequencies at 20 and 400 Hz, respectively, a 10-sampling-data-window feature extractor, and a motion classifier. Via the processing, robot motion commands can be determined, and then sent to a 6-DOF Mitsubishi RV-2A robot manipulator for execution (the specifications are listed in Table 3-4, and the axis definition is shown in Figure 3-7, only J1, J2 and J5 axes manipulated). The experimental setup is shown in Figure 3-8.

The effectiveness of the proposed scheme is demonstrated via the following two experiments: (1) 1-DOF robot arm movement governing and (2) multi-DOF robot arm movement governing. The experimental results for the former are described in Sec. 3.2, and

those for the later in Chapter 4 due to its complexity.

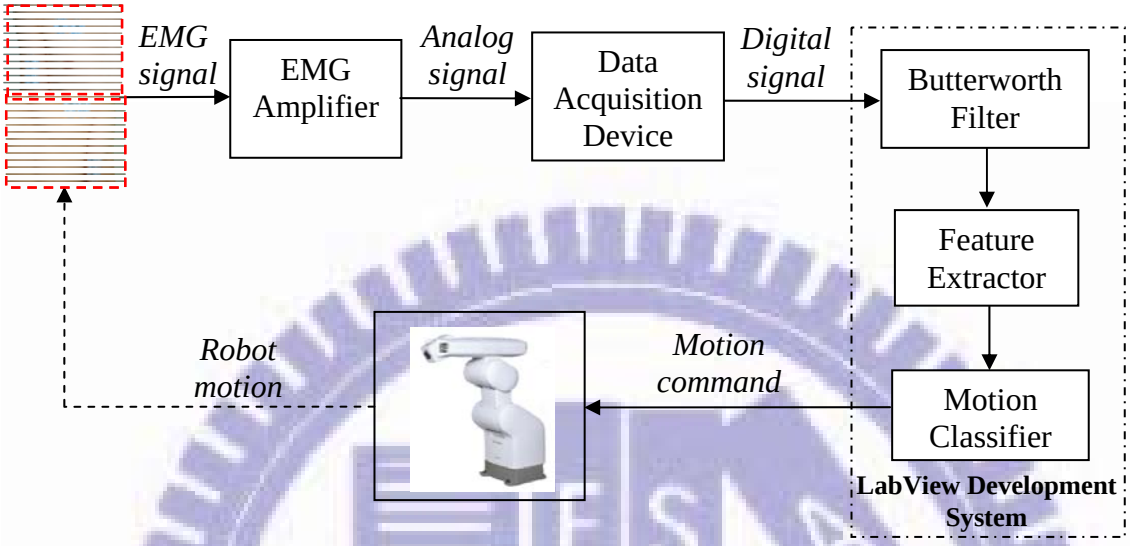

Figure 3-3 System implementation of the proposed scheme.

Table 3-2 iWork ETH-256 specifications

Number of Channel	2
Operation Modes	Bridge/Biopotential (ECG, EMG, EEG)
Gain	×1, ×5, ×10, ×100, ×500, ×1K, ×5K
Filters	High Pass (Hz): DC, 0.03, 0.3, 3 Low Pass (Hz): 5, 50, 150, 2K, 10K
Input Impedance	10 GΩ
Output Impedance	100 GΩ
Input Connector	DIN & BNC
Output Connector	BNC
Offset Range	-5 ~ +5 V
Common Mode Rejection	85db@200Hz

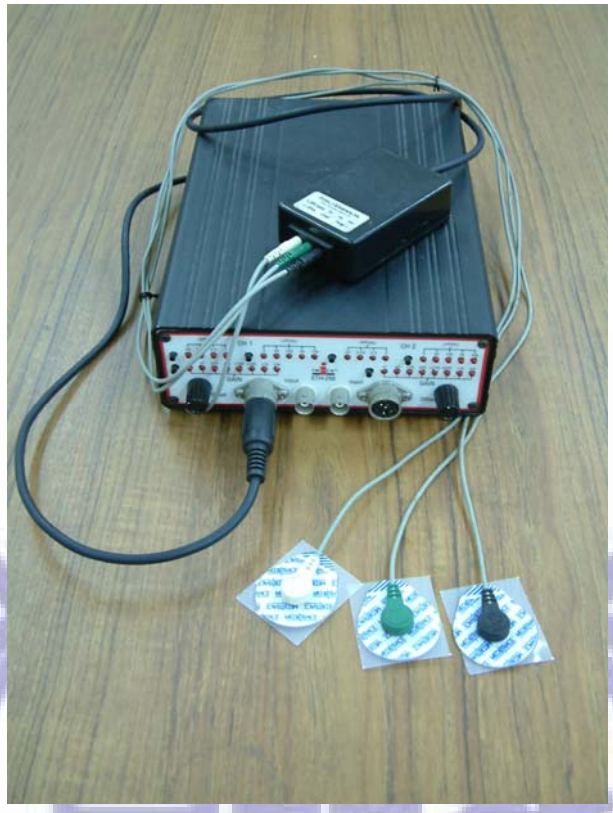

Figure 3-4 iWork ETH-256.

Table 3-3 National Instrument USB-6009 A/D data acquisition device specifications

Analog Input	Number of channel: 8 Resolution: 14 bit Sampling rate: 48 KS/s
Analog Output	Number of channel: 2 Resolution: 12 bit Sampling rate: 150 S/s
Digital I/O	Number of channel: 12 Counter: 32 bit

Figure 3-5 National Instrument USB-6009 A/D data acquisition device.

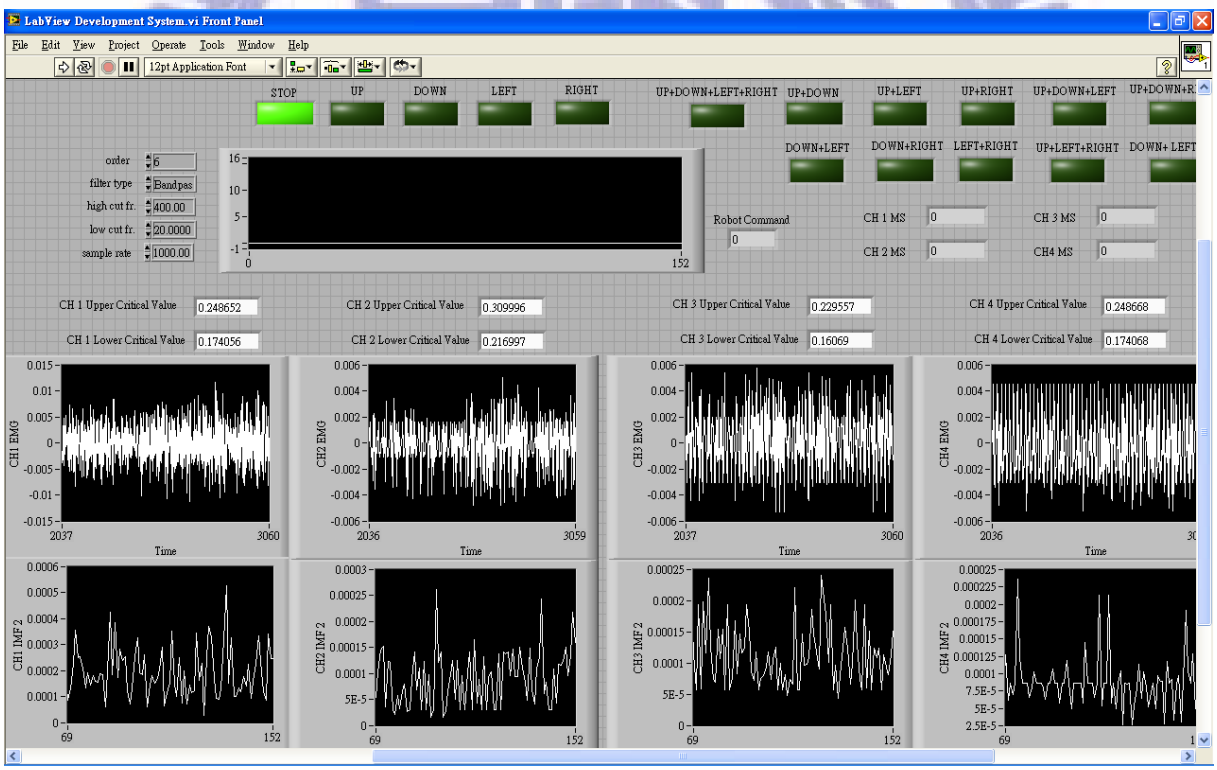

Figure 3-6 LabView Development System Console.

Table 3-4 Mitsubishi RV-2A robot arm specifications

Degrees of freedom		6
Maximum load capacity (rating)		2 Kg
Maximum reach radius		621 mm
Pose repeatability		±0.04 mm
Weight		37 Kg
Arm length	Shoulder shift	100 mm
	Upper arm	250 mm
	Fore arm	250 mm
	Elbow shift	130 mm
	Wrist length	85 mm
Operating range	J1 axis	320° (-160 to +160)
	J2 axis	180° (-45 to +135)
	J3 axis	120° (+50 to +170)
	J4 axis	320° (-160 to +160)
	J5 axis	240° (-120 to +120)
	J6 axis	400° (-200 to +200)

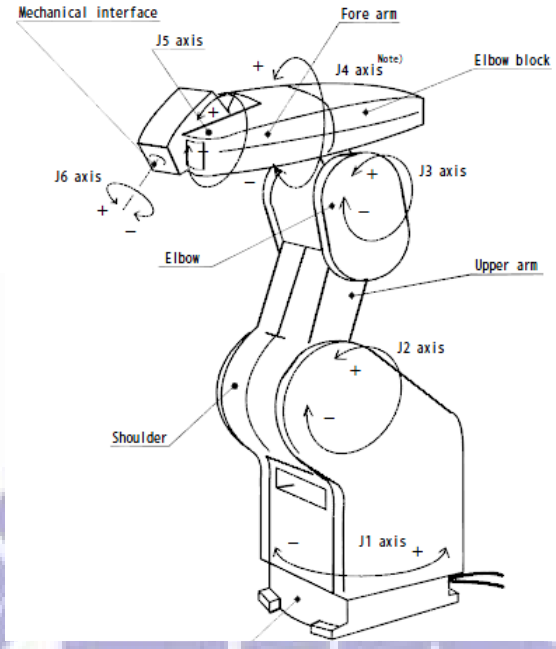

Figure 3-7 Mitsubishi RV-2A robot arm axis definition.

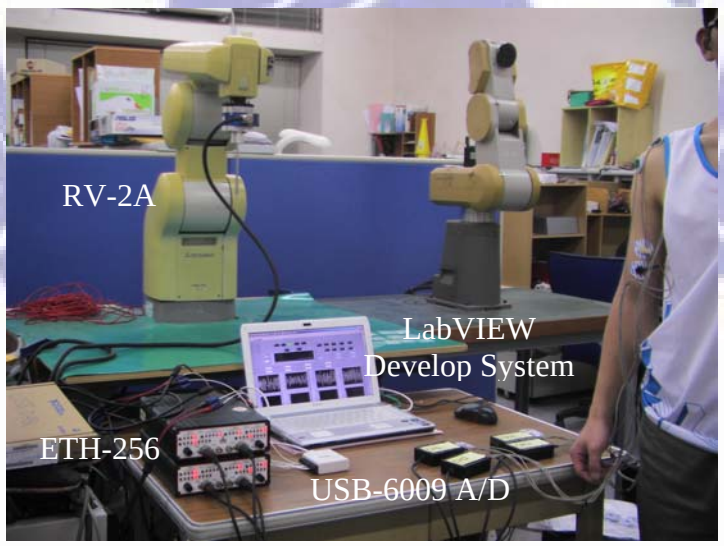

Figure 3-8 Experimental setup.

3.2 One-DOF Robot Arm Movement Control

Two sets of electrodes placed on the Biceps Brachii, marked as CH1, and the Triceps Brachii, marked CH2, respectively, shown in Figure 3-1, are used to govern the motion of RV-2A. First things first, the setting of CV_u and CV_l has to be determined for the invited subjects. In the first set of experiments, we used the empirical method to determine CV_u and CV_l for the three invited male subjects, with their physical data listed in Table 3-5 and derived CV_u and CV_l in Table 3-6. Their determination is customized for each individual subject through an extensive trial-and-error procedure according to the effectiveness on classification. The subject was asked to contract/extend his upper limb to move robot arm, J2 axis, from 0 to 90 degrees, 90 to 0 degrees, 0 to 45 degrees, 45 to 90 degrees, 90 to 45 degrees, and 45 to 0 degrees. The moving speed of the robot arm is 6 deg./sec. We define the successful discrimination rate (SDR) as the times that the robot arm successfully follows the motion of the subject out of the total number of classification:

$$SDR = \frac{\text{Number of successful motion following}}{\text{Total number of classification}} \times 100\% \qquad (3\text{-}1)$$

Table 3-5 Physical data of the three male subjects

Subject	Height (cm)	Weight (kg)	Muscle for electrode
A	174	70	Ordinary
B	166	60	Slender
C	164	82	Fat

Table 3-6 Critical values via the empirical method

Subject	Biceps Brachi		Triceps Brachi	
	CV_u	CV_l	CV_u	CV_l
A	4.5	2.2	4	2.5
B	3.2	2.2	4.5	3
C	5	2.8	5	3.3

The experimental results are shown in Figures 3-9 to 3-11. Figure 3-9 shows the EMG signals after band-pass filtering for subjects A-C, in which larger amplitudes indicate larger forces during the movements of the flexor/extensor. Figure 3-10 shows the variations of MAV features corresponding to the filtered EMG signals in Figure 3-9. Based on these features, the classifier determines the corresponding upper limb movements, while more evident feature

variations lead to better discrimination. Figure 3-11 shows the outputs from the classifier, where numbers 0-3 in the vertical coordinate denote STOP, UP, DOWN, and ERROR respectively, and I-VI the stages of 0°-90°, 90°-0°, 0°-45°, 45°-90°, 90°-45°, and 45°-0°. Subject C reported that he felt a little bit fatigued. It might be due to higher CV_u and CV_l demanded him to make more effort for movement. The SDR for the subjects is 95.5%, 97%, and 95.5%, respectively, indicating quite successful motion following.

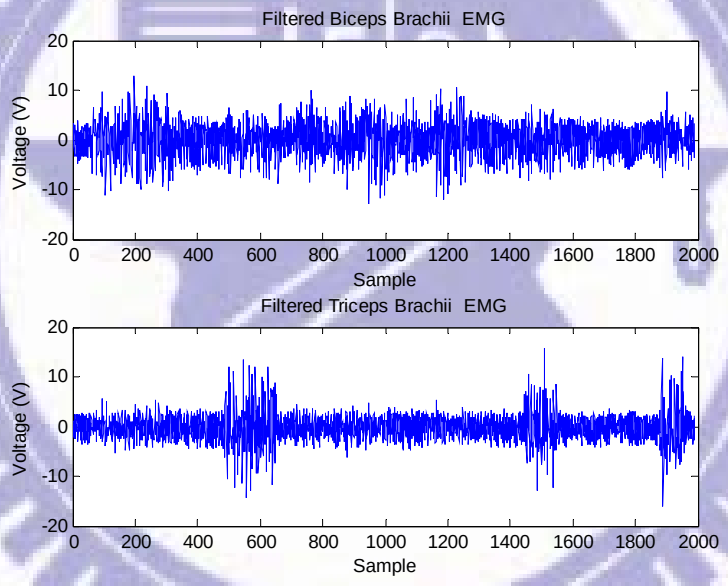

(a) Subject A

Figure 3-9 Filtered EMG signals for subjects A-C.

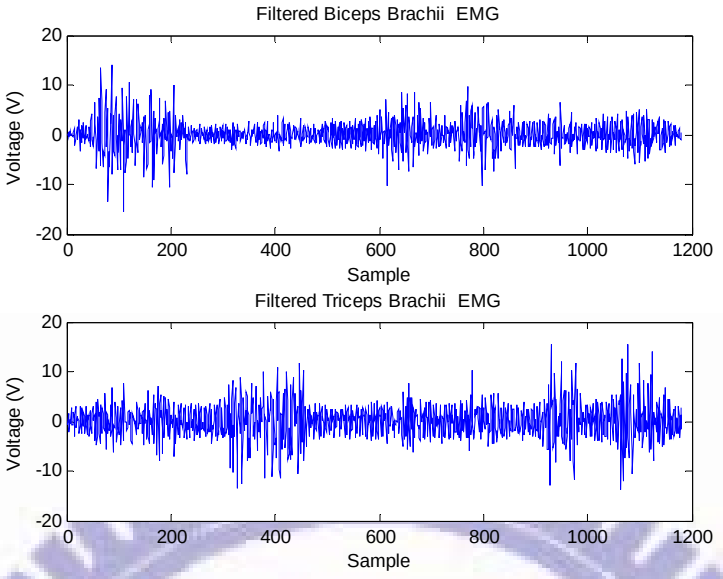

(b) Subject B

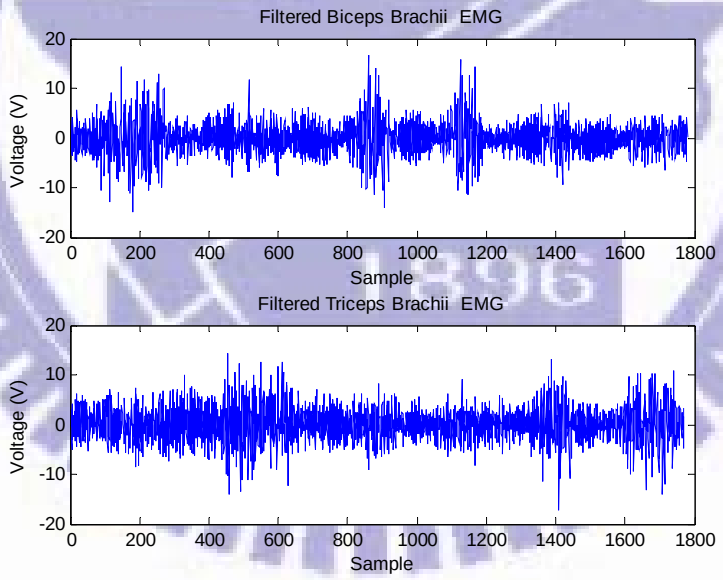

(c) Subject C

Figure 3-9 (Cont.) Filtered EMG signals for subjects A-C.

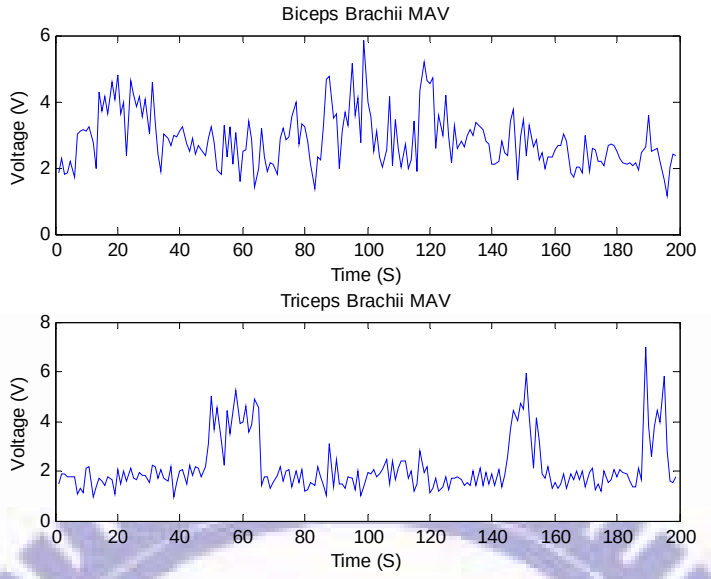

(a) Subject A

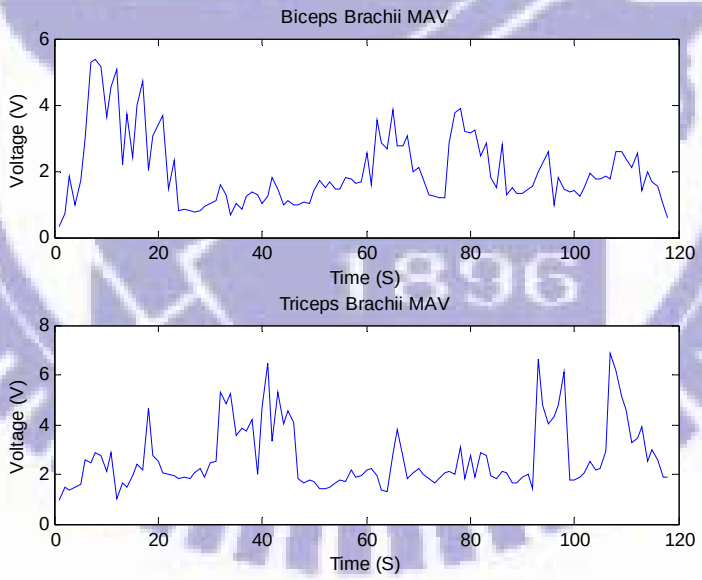

(b) Subject B

Figure 3-10 EMG feature variations for subjects A-C.

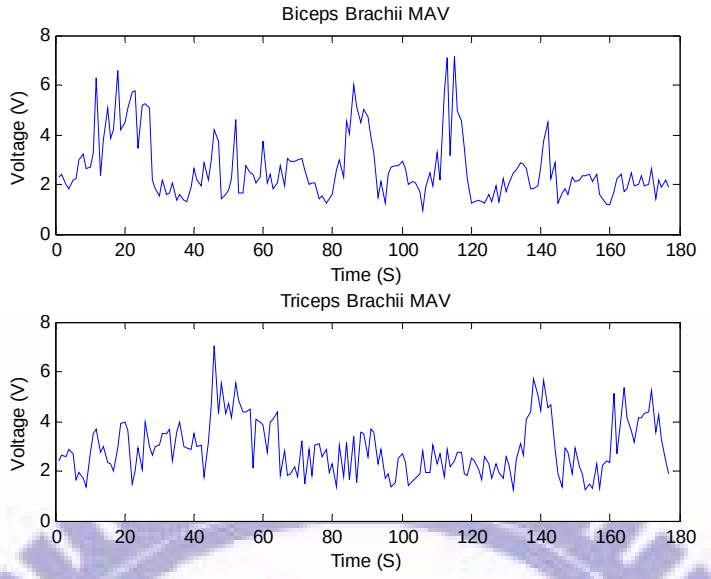

(c) Subject C

Figure 3-10 (Cont.) EMG feature variations for subjects A-C.

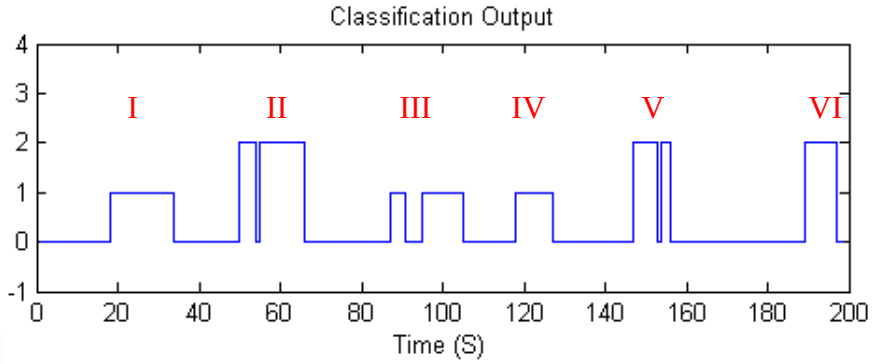

(a) Subject A

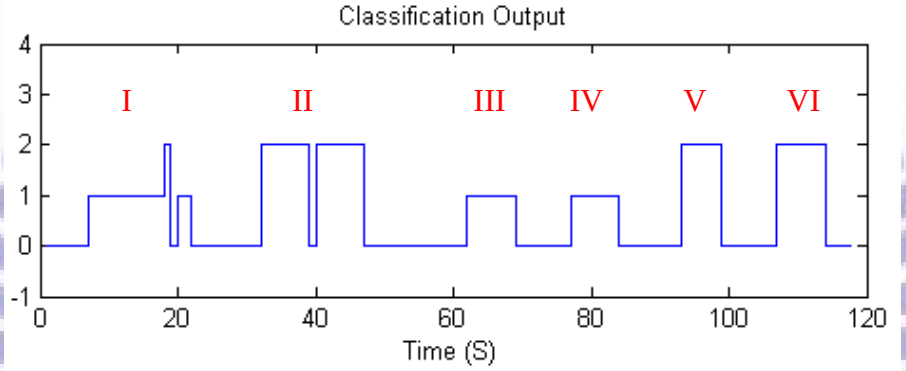

(b) Subject B

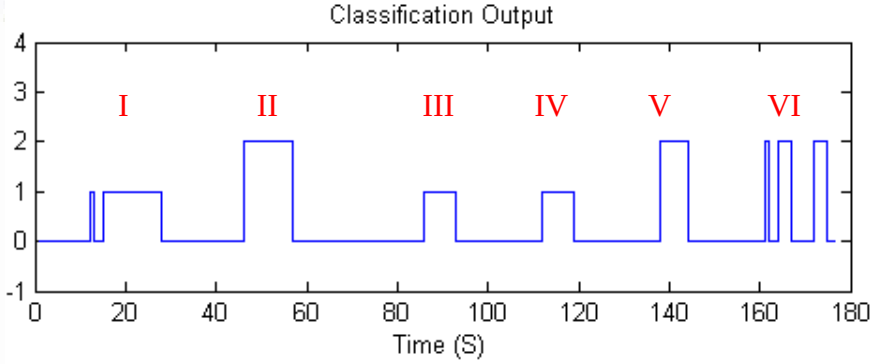

(c) Subject C

Figure 3-11 Outputs from the classifier for subjects A-C.

Due to the individual fuzziness, the tuning of the system parameters for the individual user is not that straightforward. Thus the concept of the fuzzy system [35, 51, 52] is employed for CV_u and CV_l determination, so that the tedious process encountered in the trial-and-error method can be avoided. MAV (signal power) and BZC (zero crossing) were chose as the input variables of the fuzzifier, as each of them provides the time- and frequency-domain estimation, respectively. Figure 3-12 shows the fuzzy sets used for MAV, BZC, and CV_u (CV_l), where W, M, and S stand for weak, middle, and strong, L, M, and H for low, middle, and high, γ, δ, and ε (η) the strength of MAV, BZC, and CV_u (CV_l), respectively, and $\mu_{A,}$ $\mu_{B,}$ and μ_C (μ_D) the membership function for MAV, BZC and CV_u (CV_l). With them, the fuzzifier transforms the extracted features into the linguistic values. The fuzzy rules, listed in Table 3-7, are obtained from the empirical knowledge acquired via extensive experiments. The values of γ and δ are empirically set to be 1/3 of the MAV and BZC, respectively, and ε and η are 2 and 1.4 times of γ. The fuzzy inference engine determines the *j*th firing strength α_j of the *j*th fuzzy rule via Eq.(3-2):

$$\alpha_j = \mu_{A_j} \wedge \mu_{B_j} \tag{3-2}$$

And, the defuzzifier utilizes the center of gravity (COG) method to map the inferred fuzzy action into a nonfuzzy value of CV_u (CV_l):

$$CV_u(CV_l) = \frac{\sum_{j=1}^{n} \alpha_j z_j}{\sum_{j=1}^{n} \alpha_j} \tag{3-3}$$

where n is the number of fuzzy rule and z_j the strength of CV_u (CV_l) at the jth fuzzy rule.

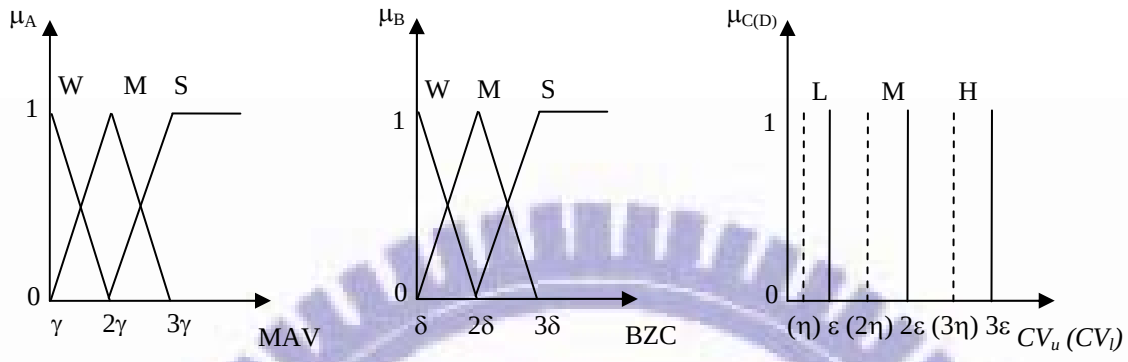

(a) MAV (b) BZC (c) CV_u (CV_l)

Figure 3-12 Fuzzy partitions of MAV, BZC, and CV_u (CV_l).

Table 3-7 Fuzzy rule base

CV_u,(CV_l)		BZC		
		W	M	S
MAV	W	L	M	M
	M	M	M	H
	S	H	H	H

In the second set of experiments, the fuzzy system is used to determine *CVs* for each individual user, listed in Table 3-8, and asked the subjects to perform the same movements as

those they did in the first set of experiments. The experimental results are shown in Figures 3-13 to 3-15. Figure 3-13 shows the filtered EMG signals, Figure 3-14 variations of the MAV features, and Figure 3-15 outputs from the classifier. The SDR for the subjects is 95.5%, 97%, and 97%, respectively, also indicating quite successful motion following. From Tables 3-6 and 3-8, different set of *CVs* were derived by the empirical method and fuzzy system, while both of them led to successful motion governing. Meanwhile, the fuzzy system may be with better potential when dealing with more complex movement, as it possesses the ability of automatic parameter tuning.

Table 3-8 Critical values via the fuzzy system

Subject	Biceps Brachi		Triceps Brachi	
	CV_u	CV_l	CV_u	CV_l
A	4.09	2.86	4.25	2.98
B	4.99	3.49	4.34	3.04
C	4.36	1.96	4.95	2.23

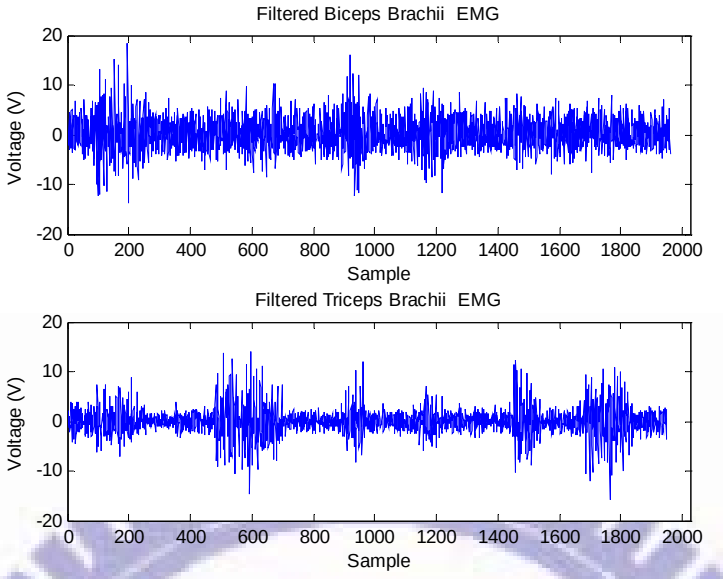

(a) Subject A

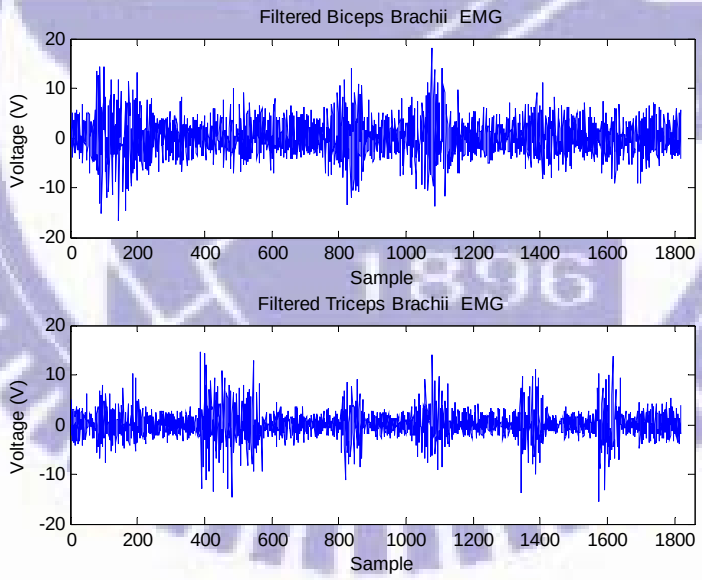

(b) Subject B

Figure 3-13 Filtered EMG signals for subjects A-C.

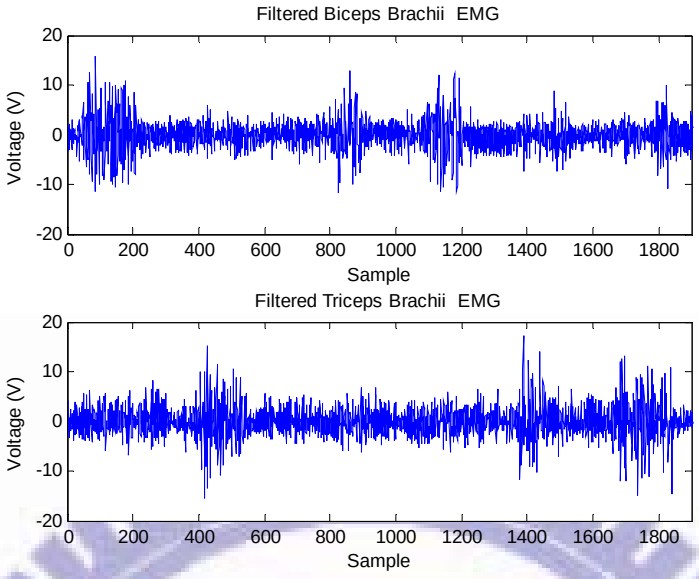

(c) Subject C

Figure 3-13 (Cont.) Filtered EMG signals for subjects A-C.

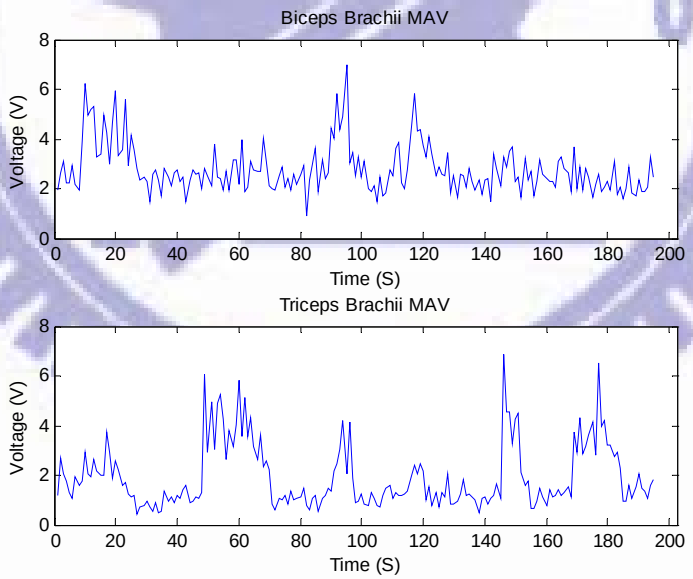

(a) Subject A

Figure 3-14 EMG feature variations for subjects A-C.

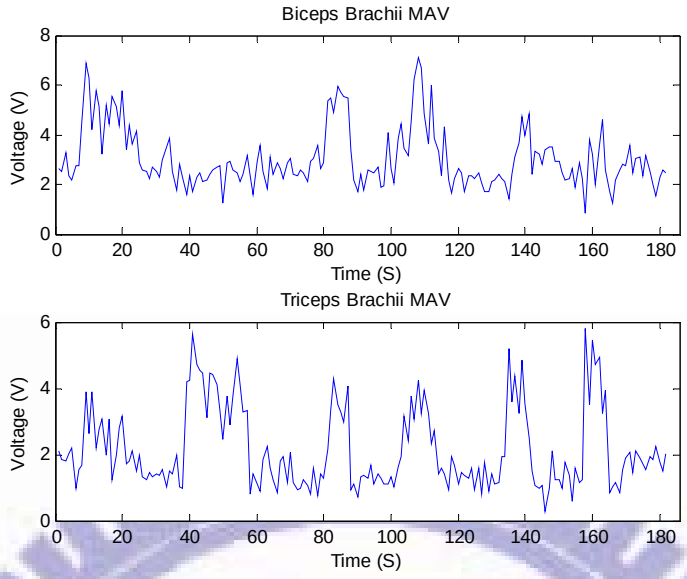

(b) Subject B

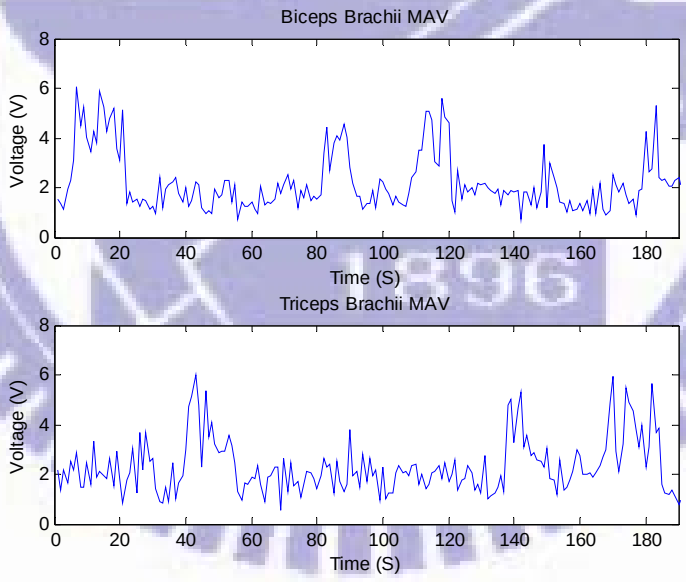

(c) Subject C

Figure 3-14 (Cont.) EMG feature variations for subjects A-C.

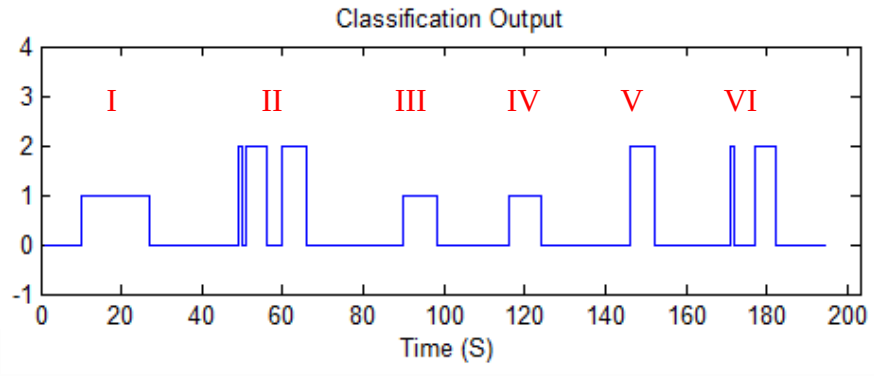

(a) Subject A

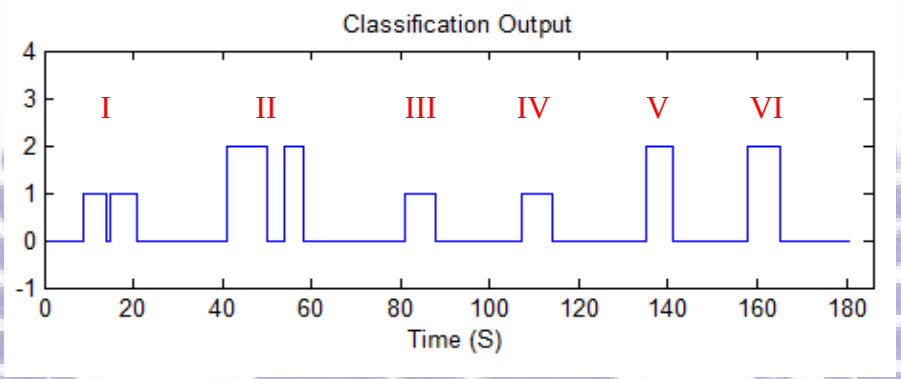

(b) Subject B

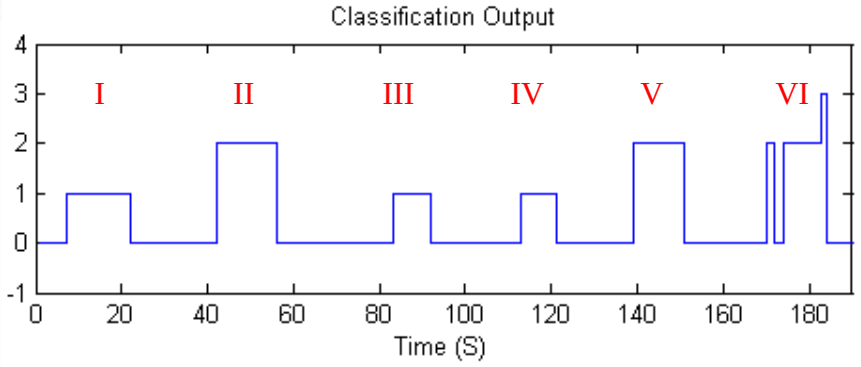

(c) Subject C

Figure 3-15 Outputs from the classifier for subjects A-C.

Chapter 4

Multi-DOF Robot Arm Movement Control

While the proposed system is shown to be effective for 1-DOF robot motion governing, it is not appropriate to serve as a classifier for more than 1-DOF upper limb motion as it has larger muscle mutual interference. To tackle this, the EMD method is applied in feature extraction design. To reduce the computational load in EMD, a sixth-order band-pass Butterworth filter and a window with 20 samples per second are employed. The muscle state was determined by the root mean square (RMS) of the 2nd IMF, $c_2(t)$, expressed as:

$$F_k = \mathrm{RMS}(c_2(t)),\ 0 \le t \le 20 \qquad (4\text{-}1)$$

Meanwhile, for multi-DOF upper limb motion, the fuzzy system adopted for 1-DOF motion is not efficient enough for the tuning of the critical values for each individual user. For its excellence on adaptation, the ANFIS is employed to realize the fuzzy system.

4.1 Adaptive Neuro-Fuzzy Inference System

Figure 4-1 shows the conceptual diagram of the proposed ANFIS for CV_u and CV_l determination, which consists of fuzzifier, fuzzy rule, fuzzy inference engine, defuzzifier and ANFIS. Fuzzifier transforms the measured EMG signals of Biceps Brachii (BB), Triceps

Brachii (TB), Pectoralis Major (PM), and Teres Minor (TM) into linguistic variables. One degree of Sugeno-type inference system is employed to depict the fuzzy rule in fuzzy inference engine. The fuzzy rules are formulated as

$$R^i: \textit{IF BB is } A_i \textit{ and TB is } B_i \textit{ and PM is } C_i \textit{ and TM is } D_i \textit{ THEN } CV_u\,(CV_l) = p_i \times \mathrm{BB} + q_i \times \mathrm{TB} + r_i \times \mathrm{PM} + s_i \times \mathrm{TM},\ i \in \{1,2,\ldots,54\} \quad (4\text{-}2)$$

where BB, TB, PM, and TM are the input variables, *A*, *B*, *C*, *D* = {W, M, S} linguistic variables, $CV_u\,(CV_l)$ the output variable, and $\begin{bmatrix} p_i & q_i & r_i & s_i \end{bmatrix}$ the consequent parameter set. Defuzzifier transforms the fuzzy results of the inference into a real $CV_u\,(CV_l)$ using weighted averaged method. ANFIS uses the least-squares method to identify the consequent parameter set and the backpropagation gradient descent method to set the premise parameters of the membership function to emulate the given training data set, listed in Table 4-1, where IN_a, IN_b, IN_c, IN_d stand for the EMG signals of BB, TB, PM and TM, respectively, OUT for CV_u, W, M, S, VL, L, H and VH for weak, middle, strong, very low, low, high and very high. By extensive experiments, the values of the W, M, S in IN_a~IN_d are empirically set to be 1/3, 2/3, 1 of IN_a~IN_d, respectively, and those of VL, L, M, H and VH in OUT are 1/3, 2/3, 1, 4/3, 5/3 of IN_a~IN_d; CV_l is set to be 0.7 times of CV_u. By considering the conditions, such as skin impedance and temperature, etc. are different from those of the training, the aforementioned values can be divided by a compensating parameter, λ, ranging from 0.8 to 1.3. The procedures for determining the CV_u and CV_l are shown in the following:

Step 1: Set the compensating parameter, λ, to be 0.8 in the proposed ANFIS to obtain the first set of CV_u and CV_l.

Step 2: Ask the operator to perform the motion of flexion, extension, internal rotation, and external rotation two times consecutively.

Step 3: If the SDR is lower than 80%, add 0.1 to λ and iterate Steps 2-3 until the SDR is equal to or more than 80%.

The proposed ANFIS consists of five layers as shown in Figure 4-2. Layer 1 is the input layer. Each node in this layer represents an input variable of the model with the membership function:

$$O_i^1 = \mu_{A_i}(BB),\ O_{i+3}^1 = \mu_{B_i}(TB),\ O_{i+6}^1 = \mu_{C_i}(PM),\ O_{i+9}^1 = \mu_{D_i}(TM),\ i = 1,2,3 \qquad (4\text{-}3)$$

The bell-shaped membership function is employed, shown in Figure 4-3, and expressed as

$$\mu_{Ai}(BB) = \frac{1}{1+\left\{\left[(BB - c_i)/a_i\right]^2\right\}^{b_i}},\quad i = 1,2,3 \qquad (4\text{-}4)$$

$$\mu_{Bi}(TB) = \frac{1}{1+\left\{\left[(TB - c_i)/a_i\right]^2\right\}^{b_i}},\quad i = 1,2,3 \qquad (4\text{-}5)$$

$$\mu_{Ci}(PM) = \frac{1}{1+\left\{\left[(PM - c_i)/a_i\right]^2\right\}^{b_i}},\quad i = 1,2,3 \qquad (4\text{-}6)$$

$$\mu_{Di}(TM) = \frac{1}{1+\left\{\left[(TM - c_i)/a_i\right]^2\right\}^{b_i}},\quad i = 1,2,3 \qquad (4\text{-}7)$$

where $[a_i \quad b_i \quad c_i]$ represent the premise parameter set. Layer 2 is the inference layer. Each node in this layer is multiplied by the input signal to become w_i:

$$O_i^2 = w_i = \mu_{Ai}(BB) \times \mu_{Bi}(TB) \times \mu_{Ci}(PM) \times \mu_{Di}(TM),\ i = 1,2,\cdots,54 \qquad (4\text{-}8)$$

w_i stands for the firing strength of the rule. Layer 3 is the normalization layer that normalizes the firing strength by calculating the ratio of i^{th} firing strength to their sum:

$$O_i^3 = \overline{w}_i = \frac{w_i}{\sum_{j=1}^{54} w_j}, \quad i = 1,2,\cdots,54 \tag{4-9}$$

Layer 4 is the output layer. Each node multiplies the normalized firing strength by the consequent function to generate the qualified consequent of each rule. The output of the node is computed as

$$O_i^4 = \overline{w}_i CV_u(CV_l)_i = \overline{w}_i\left(p_i BB + q_i TB + r_i PM + s_i TM\right), \quad i = 1,2,\cdots,54 \tag{4-10}$$

Layer 5 is the defuzzification layer, which computes the weighted average of the output signals from the output layer:

$$O_i^5 = \sum_{i=1}^{54} \overline{w}_i CV_u(CV_l)_i = \frac{\sum_{i=1}^{54} w_i CV_u(CV_l)_i}{\sum_{i=1}^{54} w_i} \tag{4-11}$$

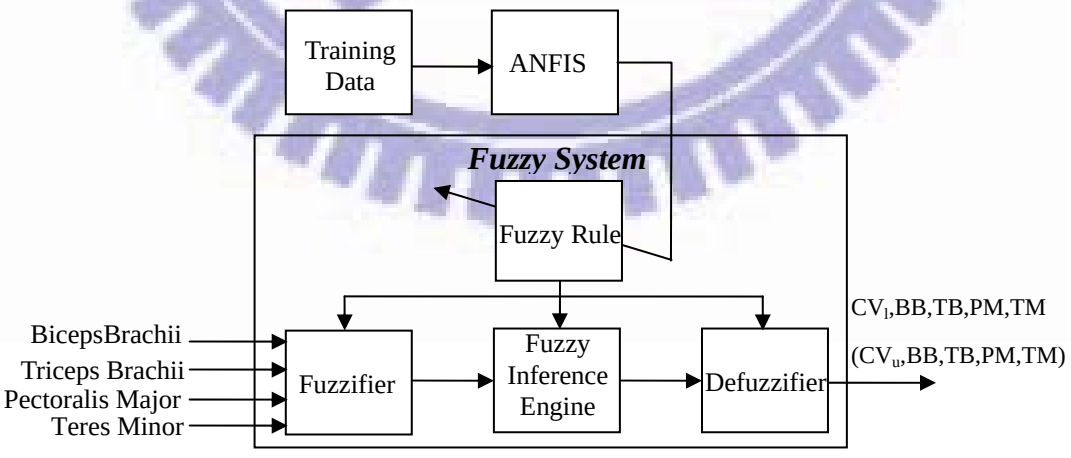

Figure 4-1 Conceptual diagram of the proposed ANFIS for CV_u and CV_l determination.

Table 4-1 Training data set

Set No.	IN_a	IN_b	IN_c	IN_d	OUT	Set No.	IN_a	IN_b	IN_c	IN_d	OUT
1	W	W	W	W	VL	**28**	M	W	W	W	L
2	W	W	W	M	VL	**29**	M	W	W	M	L
3	W	W	W	S	L	**30**	M	W	W	S	M
4	W	W	M	W	VL	**31**	M	W	M	W	L
5	W	W	M	M	L	**32**	M	W	M	M	M
6	W	W	M	S	L	**33**	M	W	M	S	M
7	W	W	S	W	VL	**34**	M	W	S	W	L
8	W	W	S	M	L	**35**	M	W	S	M	M
9	W	W	S	S	L	**36**	M	W	S	S	M
10	W	M	W	W	L	**37**	M	M	W	W	M
11	W	M	W	M	L	**38**	M	M	W	M	M
12	W	M	W	S	L	**39**	M	M	W	S	M
13	W	M	M	W	M	**40**	M	M	M	W	H
14	W	M	M	M	M	**41**	M	M	M	M	H
15	W	M	M	S	M	**42**	M	M	M	S	H
16	W	M	S	W	M	**43**	M	M	S	W	H
17	W	M	S	M	M	**44**	M	M	S	M	H
18	W	M	S	S	M	**45**	M	M	S	S	H
19	W	S	W	W	H	**46**	M	S	W	W	VH
20	W	S	W	M	H	**47**	M	S	W	M	VH
21	W	S	W	S	H	**48**	M	S	W	S	VH
22	W	S	M	W	H	**49**	M	S	M	W	VH
23	W	S	M	M	H	**50**	M	S	M	M	VH
24	W	S	M	S	H	**51**	M	S	M	S	VH
25	W	S	S	W	VH	**52**	M	S	S	W	VH
26	W	S	S	M	VH	**53**	M	S	S	M	VH
27	W	S	S	S	VH	**54**	M	S	S	S	VH

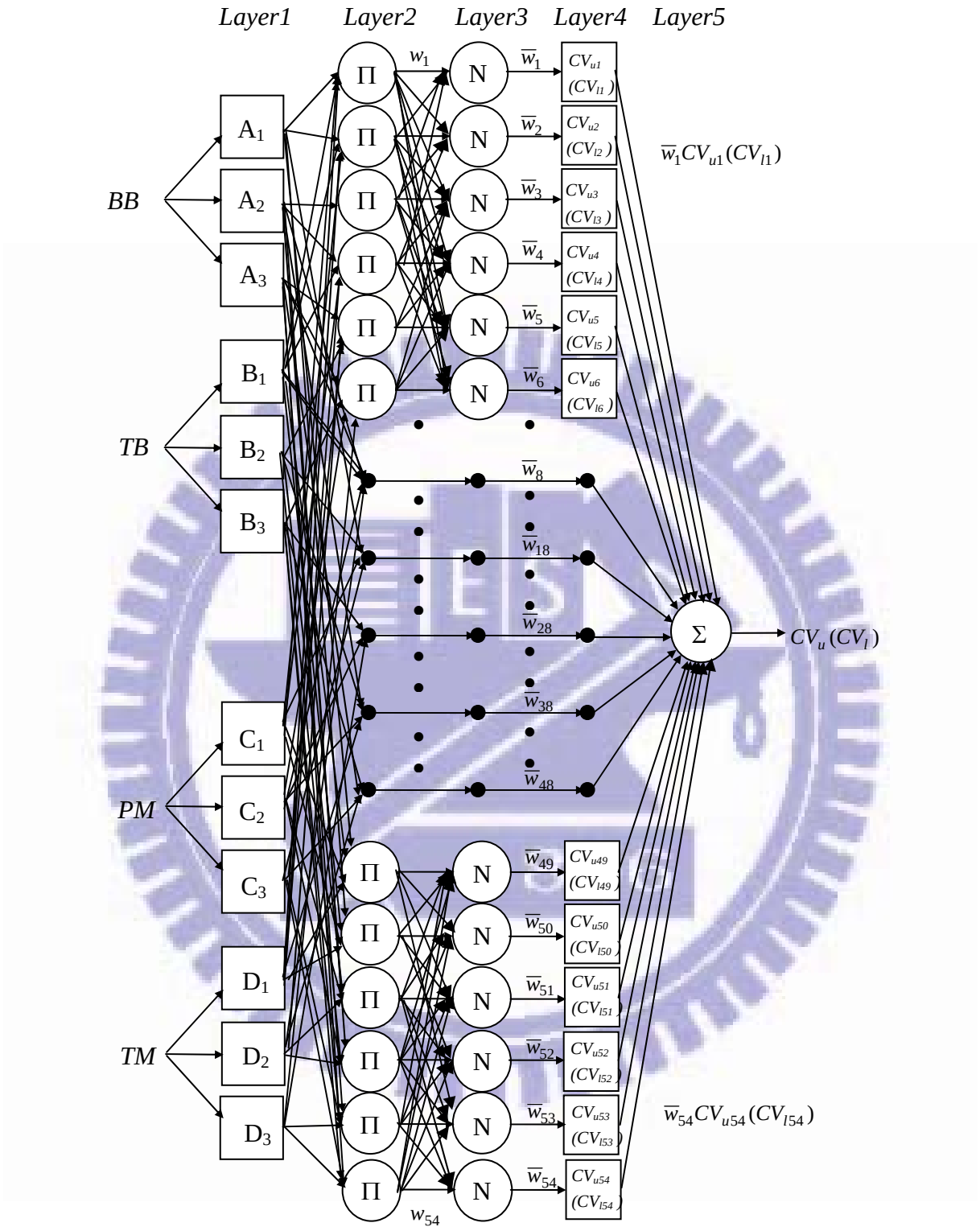

Figure 4-2 Structure of the ANFIS for the proposed system.

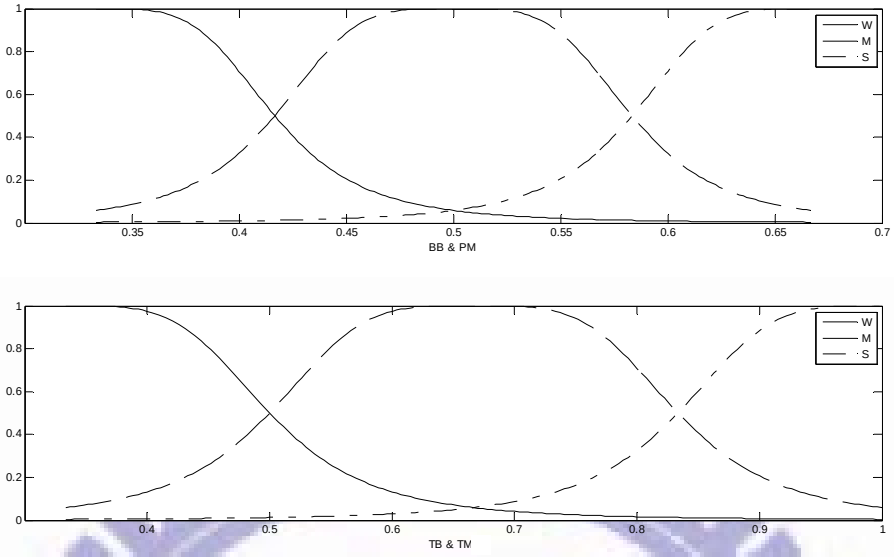

Figure 4-3 Bell-shaped membership functions for input variables.

4.2 Experimental Results

The effectiveness of the proposed scheme for governing multi-DOF robot arm movement is demonstrated via asking two male and two female subjects (with their physical data listed in Table 4-2) to perform the following three experiments: (1) the motion of flexion, extension, internal rotation, and external rotation for four times consecutively, (2) the motion of flexion plus internal rotation, and extension plus external rotation for three times consecutively, and (3) the motion of elbow up, down, internal rotation, external rotation, flexion plus internal rotation, and extension plus external rotation for two times consecutively. Experiment 1 is used to check the feasibility of the proposed system for recognizing several multi-DOF upper

limb motions, experiment 2 to check the capability of the proposed system for recognizing the motion with larger muscle mutual interference, and experiment 3 to evaluate the operation duration of the proposed system.

Table 4-2 Physical data of the four subjects

Subject	Height (cm)	Weight (kg)	Gender	Muscle for electrode
A	166	60	Male	Slender
B	164	82	Male	Fat
C	155	52	Female	Ordinary
D	150	50	Female	Ordinary

4.2.1 Experiment 1

The results for experiment 1 are shown in Figure 4-4 which includes the subject's CH1-4 filtered raw EMG signals, CH1-4 muscle states, and the classification output. The muscle states reveal that subjects C and D had significantly mutual muscle interferences occurred during movements, especially subject D. The SDR for the subjects is 97%, 100%, 87.9%, and 81.8%, respectively. The proposed system still achieved quite high a successful discrimination rate for subject D though.

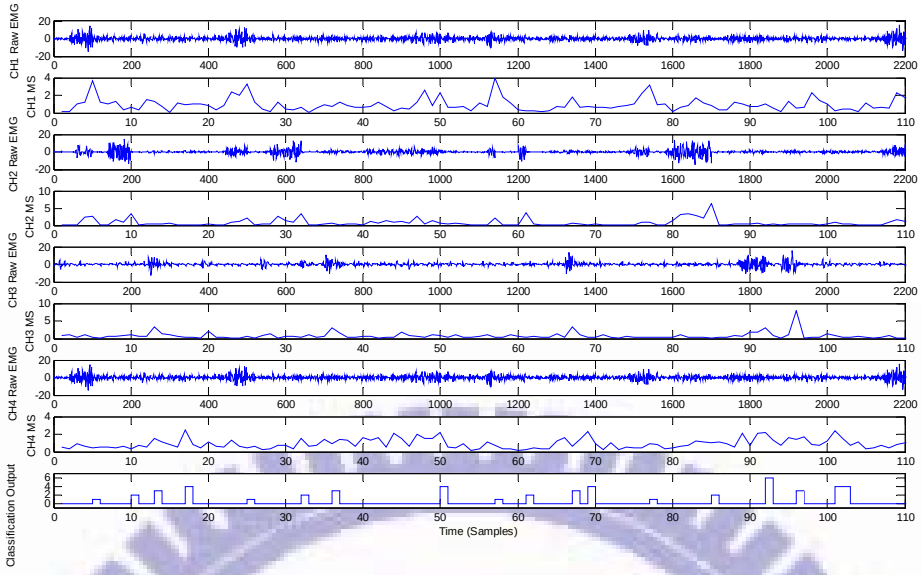

(a) Subject A

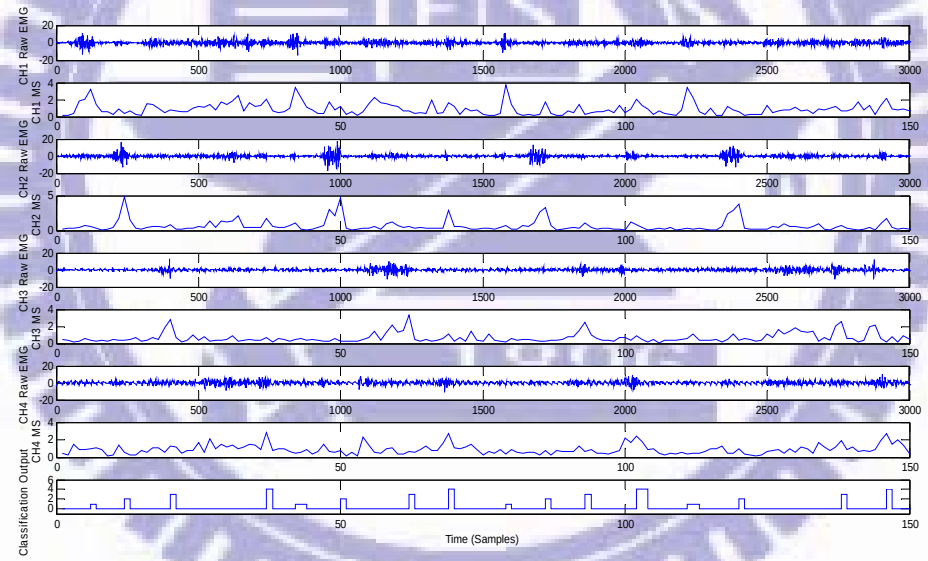

(b) Subject B

Figure 4-4 Results for experiment 1.

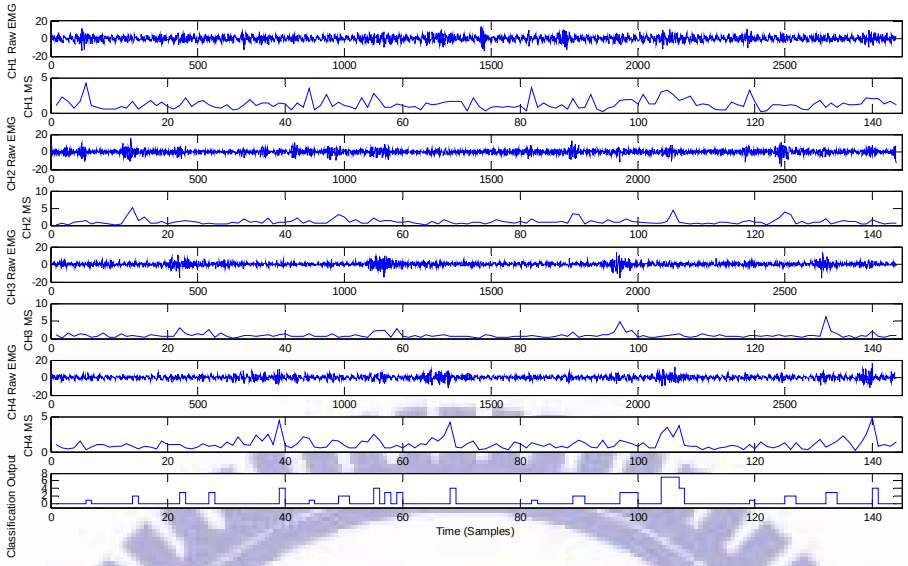

(c) Subject C

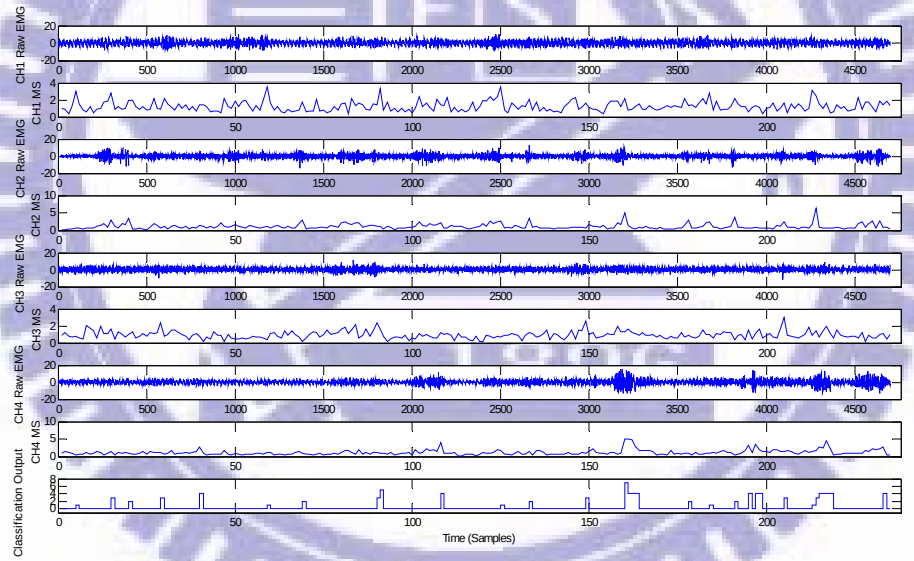

(d) Subject D

Figure 4-4(Cont.) Results for experiment 1.

4.2.2 Experiment 2

Different from the motions performed in experiment 1, the motions in experiment 2 are determined via detecting the instant when both magnitudes of the extracted BB and PM (TB and TM) reach their individual upper critical value simultaneously. These motions led to not only larger mutual muscle interferences but also higher muscle coupling. The experimental results are shown in Figure 4-5. The muscle states reveal that the subjects' forces acting on BB and PM (TB and TM) sometimes did not reach individual upper critical value simultaneously. Nevertheless, the goal was still achieved, and the SDR for the subjects is 84.6%, 92.3%, 76.9%, and 100%, respectively, indicating that the proposed system dealt with these complicated motions successfully.

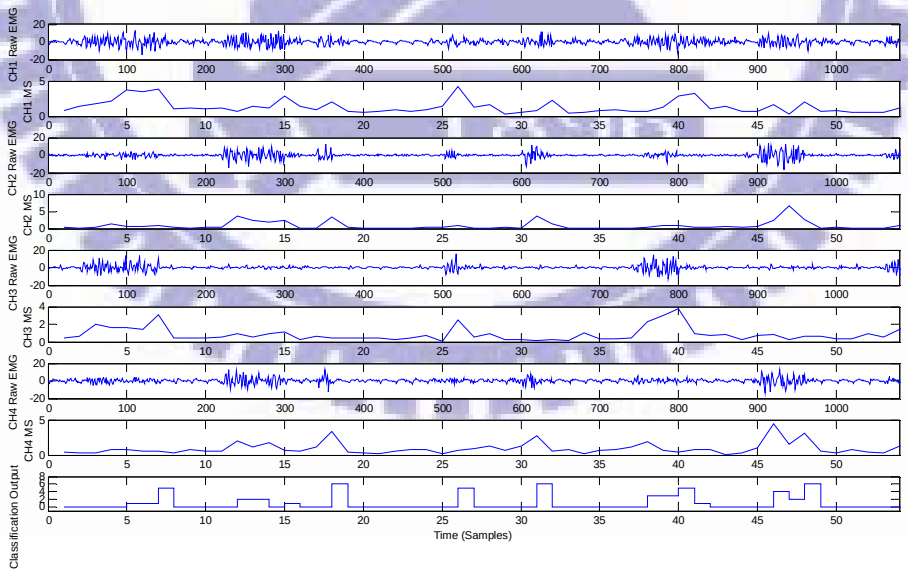

(a) Subject A

Figure 4-5 Results for experiment 2.

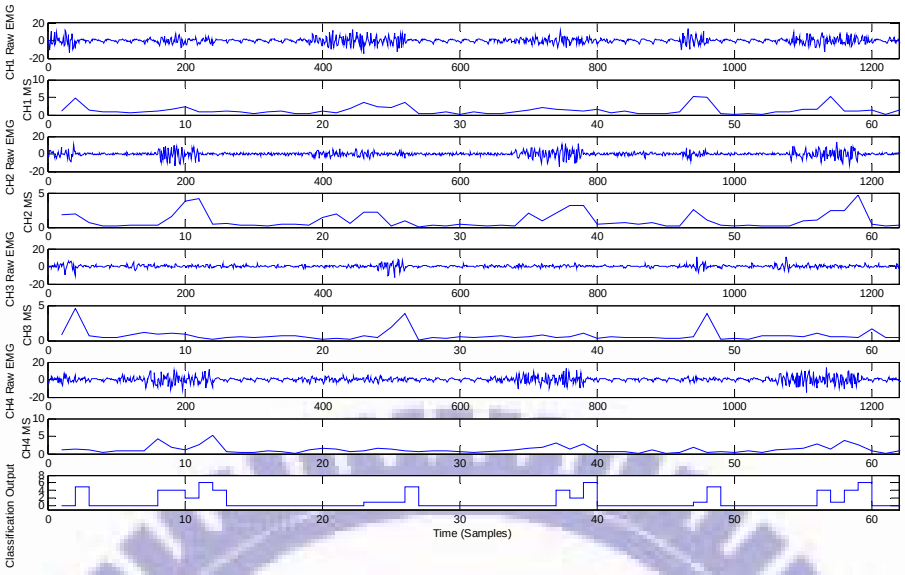

(b) Subject B

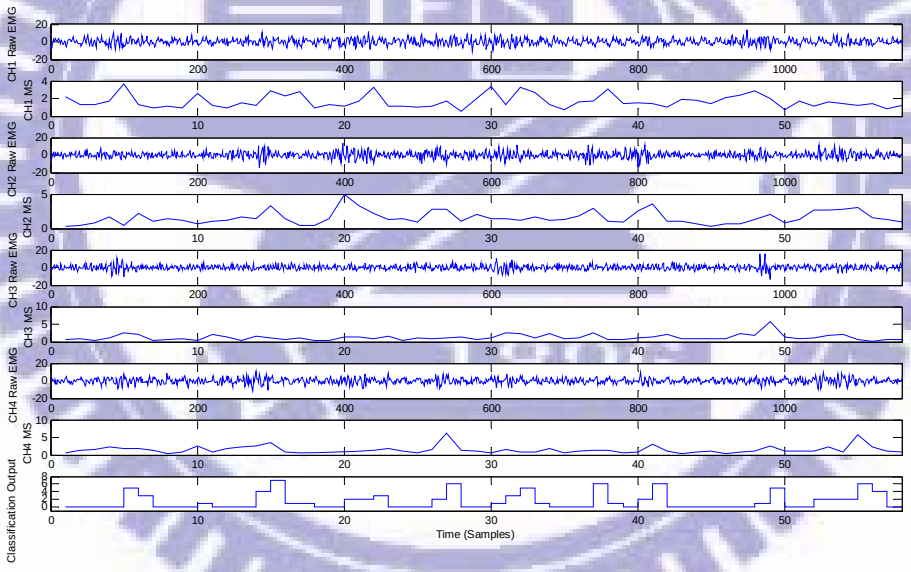

(c) Subject C

Figure 4-5 (Cont.) Results for experiment 2.

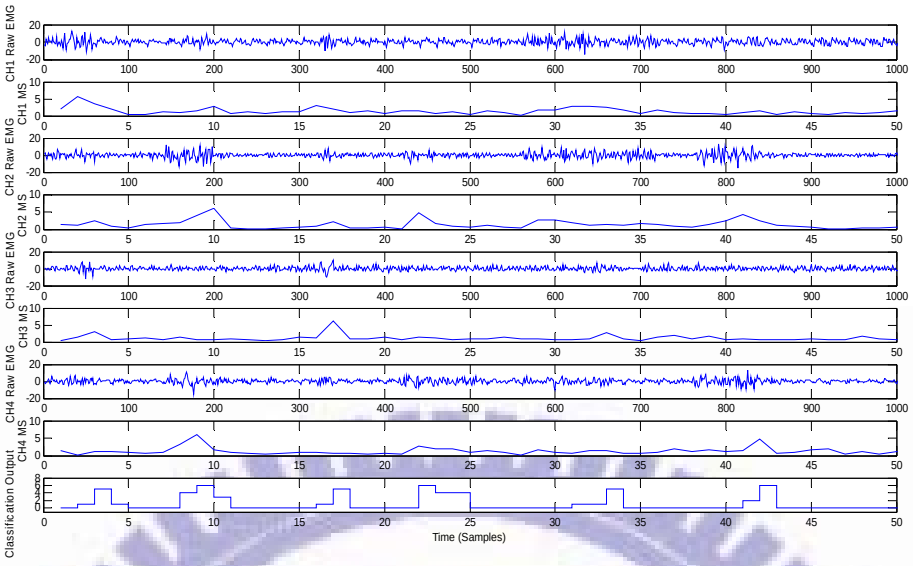

(d) Subject D

Figure 4-5 (Cont.) Results for experiment 2.

4.2.3 Experiment 3

To evaluate the operation duration of the proposed system, we asked the subjects to perform the motion of elbow up, down, internal rotation, external rotation, flexion plus internal rotation, and extension plus external rotation continuously. In average, the subjects felt fatigued after continuously executing the motions twice. The results for experiment 3 are shown in Figure 4-6. The SDR for the subjects is 96%, 92%, 72%, and 84%, respectively, indicating quite successful motion following except for subject C. When examining the muscle state of subject C, we found the severe mutual muscle interference present in her

motion of extension plus external rotation.

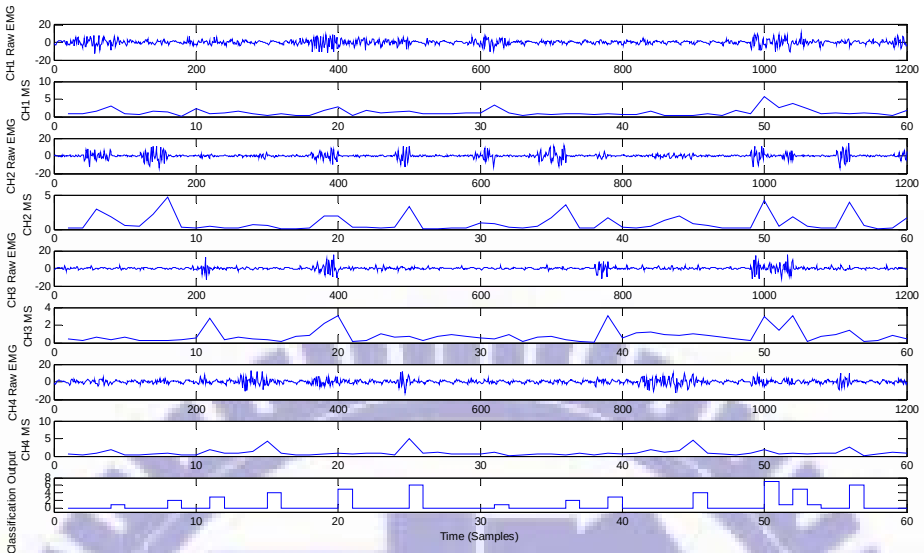

(a) Subject A

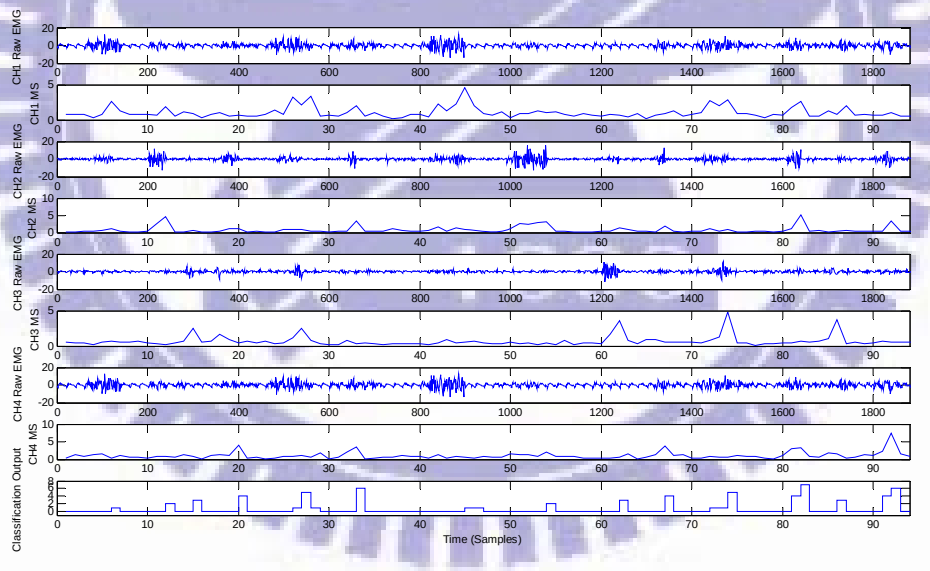

(b) Subject B

Figure 4-6 Results for experiment 3.

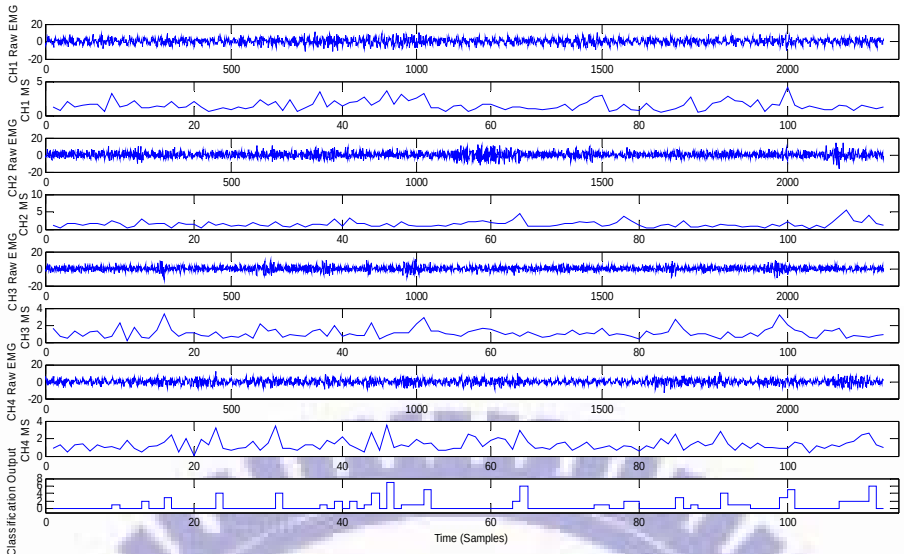

(c) Subject C

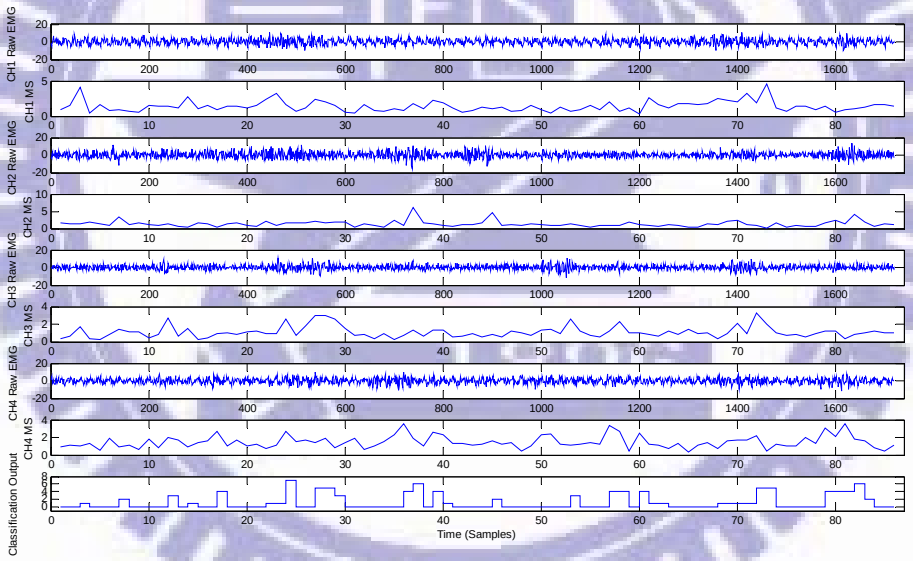

(d) Subject D

Figure 4-6 (Cont.) Results for experiment 3.

Chapter 5
Conclusions

The main aim of the dissertation is proposing a simple and practicable approach, a so-called initial point detection method, to discriminate the upper limb motion onset by detecting the instant when the magnitude of the extracted EMG feature reaches the upper critical value CV_u and offset when that descends to the lower critical value CV_l from onset state. By integrating the method with the EMD and the fuzzy system, the mapping between the upper limb EMG signals and the corresponding robot arm movements can be established very quickly and reliable. A series of experiments have been performed to demonstrate the feasibility and effectiveness of the proposed system. Because neither complicated computation nor training and learning processes are needed, the proposed scheme not only simplifies system complexity, but also increases the efficiency in motion governing. With the assistance of the proposed system, the physically weak individual (disabled, injured or elderly) can do some important daily activities such as eating from spoon, drinking from cup and pouring from a bottle, etc. by themselves without needing assistance from others. In addition to the robot arm motion governing, the proposed method can further be used for governing the different fundamental applications, such as the devices with bidirectional commands (on/off, increment/decrement), prosthetic hand, TV and radio for instance.

Although the experimental results demonstrate the feasibility of the proposed system, the

classifier can not recognize the state while the forces acting two muscles (BB and PM or TB and TM) do not reach individual upper critical value simultaneously. Meanwhile, its performance has not yet been evaluated by the physically handicapped and elderly. The muscle contractions in these people will often be very weak so that the magnitudes of their EMG signals might be lower than those of the background noises. The feature extractor and the fuzzy rules used for the subjects with sound limbs would not be suitable for them and need to be modified. Besides, the proposed system can not control the position of the robot arm because to develop an EMG based human-assisting manipulator with a controller that accurately controls the position requires not only more sensing instruments but also the muscular model, which increases the loading of signal measurement and processing as well as system complexity.

5.1 Future Research

While the experimental results are shown to be effective for robot motion governing, the limitation of this system is that fixed *CVs* are suitable for robot motion governing for about 5 ~ 10 minutes, depending on the complexity of the motion. After that, the fatigue of the muscle led to inconsistent classification. Consequently, the proposed system should not be used when the subject feels fatigued. Besides, the movements involved in the proposed system only focus on the upper limb motions, and the subjects are all sound limbs and younger. Whether it is suitable for governing full limb movements and operating by physically weak individual remain to be investigated. In future works, we plan to lengthen the operation time by adopting the strategy of varying *CVs* with the detection of the fatigue in the system. We also plan to extend the proposed system for full limb movement governing. In addition, we also demonstrate the performance of the proposed system for subjects that are the physically handicapped and with age.

Bibloigraphy

[1] K. Watanabe, C. Jayawardena, and K. Izumi, “Intelligent interface using natural voice and vision for supporting the acquisition of robot behaviors,” IEEE International Conference on Sensors, pp. 374-377, Oct. 2006.

[2] C. J. D. Luca, “The use of surface electromyography in biomechanics”, Journal of Applied Biomechanics, vol. 13, no. 2, pp. 135-163, 1997.

[3] O. Fukuda, T. Tsuji, M. Kaneko, and A. Otsuka, “A human-assisting manipulator teleoperated by EMG signals and arm motions,” IEEE Transactions on Robotics and Automation, vol. 19, no. 2, pp. 210-222, Apr. 2003.

[4] P. K. Artemiadis and K. J. Kyriakopoulos, “EMG-based position and force control of a robot arm: application to teleoperation and orthosis,” IEEE/ASME International Conference on Advanced Intelligent Mechatronics, pp. 1-6, Sep. 2007.

[5] A. Ferreira, W. C. Celeste, F. A. Cheein, T. F. Bastos-Filho, M. Sarcinelli-Filho, and R. Carelli, “Human-machine interfaces based on EMG and EEG applied to robotic systems,” Journal of NeuroEngineering and Rehabilitation, vol. 5, no. 10, pp. 1-15, Mar. 2008.

[6] Z. Gao, Q. Song, Y. Nie, J. Lei, Y. Yong, and Y. Ge, “Conceptual design and implementation of arm wrestling robot,” IEEE/RSJ International Conference of

Intelligent Robots and Systems, pp. 4582-4586, Oct. 2006.

[7] R. A. R. C. Gopura and K. Kiguchi, “EMG-based control of an exoskeleton robot for human forearm and wrist motion assist,” IEEE International Conference on Robotics and Automation, pp. 731-736, May 2008.

[8] K. Ito, T. Tsuji, A. Kato, and M. Ito, “An EMG-controlled prosthetic forearm in three degrees of freedom using ultrasonic motors,” Proceedings of the Annual International Conference of the IEEE Engineering in Medicine and Biology Society, pp. 1487–1488, Nov. 1992.

[9] H. Oppenheim, R. S. Armiger, and R. J. Vogelstein, "WiiEMG: a real-time environment for control of the Wii with surface electromyography," Proceedings of IEEE International Symposium on Circuits and Systems, pp. 957 – 960, Jun. 2010.

[10] H. Huang, T. A. Kuiken, and R. D. Lipschutz, “Strategy for identifying locomotion modes using surface electromyography,” IEEE Transaction on Biomedical Engineering, vol. 56, no.1, pp. 65-73, Jan. 2009.

[11] S. Aso, A. Sasaki, and H. Hashimoto, “Driving electric car by using EMG interface,” IEEE Conference on Cybernetics and Intelligent Systems, pp. 1-5, Jun. 2006.

[12] A. Harada, T. Nakakuki, M. Hikita, and C. Ishii, ”Robot finger design for myoelectric hand and recognition of finger motions via Surface EMG,” IEEE Conference on Automation and Logistics, pp. 273-278, Aug. 2010.

[13] H. Graichen, K. H. Englmeier, M. Reiser, and F. Eckstein, “An in vivo technique for determining 3D muscular moment arms in different joint positions and during muscular activation – application to the supraspinatus,” Clinical Biomechanics, vol. 16, no. 5, pp. 389–394, June. 2001.

[14] K. Kiguchi, T. Tanaka, and T. Fukuda, “Neuro-fuzzy control of a robotic exoskeleton with EMG signals,” IEEE Transactions on Fuzzy Systems, vol. 12, no. 4, pp. 481-490, Aug. 2004.

[15] A. Soares, A. Andrade, E. Lamounter, and R. Carrijo, “The development of a virtual myoelectric prosthesis controlled by an EMG pattern recognition system based on neural networks,” Journal of Intelligent Information Systems, vol. 21, no. 2, pp. 127-141, 2003.

[16] M. Z. Kermani, B. C. Wheeler, K. Badie, and R. M. Hashemi, “EMG feature evaluation for movement control of upper extremity prostheses,” IEEE Transaction on Rehabilitation Engineering, vol. 3, no. 4, pp. 324-333, Dec. 1995.

[17] H. P. Huang and C. Y. Chen, “Development of a myoelectric discrimination system for a multi-degree prosthetic hand,” Proceedings of IEEE International Conference on Robotics and Automation, pp. 2392-2397, May 1999.

[18] Y. Li, Y. Tian and W. Chen, “Multi-pattern recognition of sEMG based on improved BP neural network algorithm,” Proceedings of the 29th Chinese Control Conference, pp. 2867-2872, Jul. 2010.

[19] A. Phinyomark, S. Hirunviriya, C. Limsakul, and P. Phukpattaranont, “Evaluation of EMG feature extraction for hand movement recognition based on Euclidean distance and standard deviation,” International Conference on Electrical Engineering/Electronics Computer Telecommunications and Information Technology, pp. 856 – 860, May 2010.

[20] M. Meng, Q. She, Y. Gao, and Z. Luo, “EMG signals based gait phases recognition using hidden Markov models,” IEEE International Conference on Information and Automation, pp. 852-856, Jun. 2010.

[21] J. Gora, P. M. Szecowka, and A. R. Wolczowski, “Control of dexterous hand - algorithm implementation issues,” International Conference on Information Technology and Applications in Biomedicine, pp. 1-4, Nov. 2009.

[22] S. Karlsson, J. Yu, and M. Akay, “Enhancement of spectral analysis of myoelectric signals during static contractions using wavelet methods,” IEEE Trans. Biomed. Eng. vol. 46, pp. 670-684, Jun. 1999.

[23] K. Mahaphonchaikul, D. Sueaseenak, C. Pintavirooj, M. Sangworasil, and S. Tungjitkusolmun, “EMG signal feature extraction based on wavelet transform,” International Conference on Electrical Engineering/Electronics Computer Telecommunications and Information Technology, pp. 327 – 331, May 2010.

[24] H. Xie and Z. Wang, “Mean frequency derived via Hilbert-Huang transform with application to fatigue EMG signal analysis,” Computer Methods and Programs in

Biomedicine, vol. 82, pp. 114-120, 2006.

[25] C. Zong and M. Chetouani, “Hilbert-Huang transform based physiological signals analysis for emotion recognition,” IEEE International Symposium on Signal Processing and Information Technology, pp. 334-339, Dec. 2009.

[26] A. O. Andrade, S. Nasuto, P. Kyberd, C. M. Sweeney-Reed, and F. R. Van Kanijn,” EMG signal filtering based on empirical mode decomposition,” Biomedical Signal Processing and Control, vol. 1, pp. 44-45, 2006.

[27] P. Afshar and Y. Matsuoka, “Neural-based control of a robotic hand: evidence for distinct muscle strategies,” Proceedings of IEEE International Conference on Robotics and Automation, pp. 4633-4638, May 2004.

[28] N. Bu, M. Okamoto, and T. Tsuji, “A hybrid motion classification approach for EMG-based human-robot interfaces using Bayesian and neural networks,” IEEE Transactions on Robotics, vol. 25, no. 3, pp. 502-511, Jun. 2009.

[29] W. Ma and Z. Luo, “Hand-motion pattern recognition of sEMG based on Hilbert-Huang transformation and AR-model,” IEEE International Conference on Mechatronics and Automation, pp. 2150-2154, Aug. 2007.

[30] B. Peng, X. Jin, Y. Min, and X. Su, “The study on the sEMG signal characteristics of muscular fatigue base on the Hilbert-Huang transform,” Lecture Notes in Computer Science, vol. 3991, pp. 140-147, 2006.

[31] N. Wang, E. Ambikairajah, B. G. Celler, and N. H. Lovell, “Accelerometry based classification of gait patterns using empirical mode decomposition,” IEEE International Conference on Acoustics, Speech, and Signal Processing, pp. 617-620, Apr. 2008.

[32] L. Chen, P. Yang, L. Zu, and X. Guo, “Movement recognition by electromyography signal for transfemoral prosthesis control,” IEEE Conference on Industrial Electronics and Applications, pp. 1127-1132, May 2009.

[33] P. K. Artemiadis and K. J, Kyriakopoulos, “A switching regime model for the EMG-based control of a robot arm,” IEEE Transactions on Systems, Man, and Cybernetics-Part B: Bybernetics, vol. 41, no. 1, pp. 53-63, Feb. 2011.

[34] H. J. Liu and K. Y. Young, “An Adaptive Upper arm EMG-based robot control system,” International Journal of Fuzzy Systems, vol. 12, no. 3, pp. 181-189, Sep. 2010.

[35] H. J. Liu and K. Y. Young, “An efficient approach for EMG-based robot control,” International Journal of Electrical Engineering, vol. 17, no. 5, pp. 327-336, Oct. 2010.

[36] C. A. Chen, H. K. Chiang, and J. C. Shen, “Fuzzy sliding mode control of a magnetic ball suspension system”, International Journal of Fuzzy Systems, vol. 11, no. 2, pp. 97-106, Jun. 2009.

[37] C. H. Wang, C. H. Lin, B. K. Lee, C. N. Liu, and C. Su, “Adaptive two-stage fuzzy temperature control for an electroheat system”, International Journal of Fuzzy Systems, vol. 11, no. 1, pp. 59-66, Mar. 2009.

[38] H. Y. Chan, Y. S. Yang, F. K. Lam, Y. T. Zhang, and P. A. Parker, “Fuzzy EMG classification for prosthesis control,” IEEE Transactions on Rehabilitation Engineering, vol. 8, no. 3, pp. 305-311, Sep. 2000.

[39] J. S. R. Jang, “ANFIS: Adaptive network based fuzzy inference system,” IEEE Transactions on Systems, Man, and Cybernetics, vol. 23, no. 3, pp. 665-683, May/Jun. 1993.

[40] B. K. Lee, K. H. Lee, and B. S. Chen, “State estimation of stochastic T-S fuzzy systems,” International Journal of Fuzzy Systems, vol. 8, no. 1, pp. 46-56, Mar. 2006.

[41] C. Y. Kuo and H. F. Wang, “Overview of fuzzified neural networks with comparison of learning mechanism,” International Journal of Fuzzy Systems, vol. 10, no. 2, pp. 71-83, Jun. 2008.

[42] M. J. Er, F. Liu, and M. B. Li, “Self-constructing fuzzy neural networks with extended Kalman filter,” International Journal of Fuzzy Systems, vol. 12, no. 1, pp. 66-72, Mar. 2010.

[43] A. Subasi, “Application of adaptive neuro-fuzzy inference system for epileptic seizure detection using wavelet feature extraction,” Computers in Biology and Medicine, vol. 37, no. 2, pp. 227-244, 2007.

[44] C. K. S. Vijila, P. Kanagasabapathy, S. Johnson, and V. Ewards, “Artifacts removal in EEG signal using adaptive neuro fuzzy inference system,” IEEE International

Conference Signal Processing, Communications and Networking, pp. 589-591, Feb. 2007.

[45] S. Micera, W. Jensen, F. Sepulveda, R. R. Riso, and T. Sinkjær, “Neuro-fuzzy extraction of angular information from muscle afferents for ankle control during standing in paraplegic subjects: an animal model,” IEEE Transactions on Biomedical Engineering, vol. 48, no. 7, pp. 787-794, Jul. 2001.

[46] R. T. Lauer, B. T. Smith, and R. R. Betz, “Application of a neuro-fuzzy network for gait event detection using electromyography in the child with cerebral palsy,” IEEE Transactions on Biomedical Engineering, vol. 52, no. 9, pp. 1532-1540, Sep. 2005.

[47] J. I. Park, J. H. Cho, M. G. Chun, and C. K. Song, “Neruo-fuzzy rule generation for backing up navigation of car-like mobile robots,” International Journal of Fuzzy Systems, vol. 11, no. 3, pp. 192-201, Sep. 2009.

[48] M. Y. Shieh and K. H. Chang, “An optimized neuro-fuzzy controller design for bipedal locomotion,” International Journal of Fuzzy Systems, vol. 11, no. 3, pp. 137-145, Sep. 2009.

[49] K. Henryk, S. Grzegorz , and N. Anton, "Effect of Electrode Position on EMG Recording in Pectoralis Major," Journal of Human Kinetics, vol.17, pp. 105-112, 2007.

[50] N. E. Huang, S. Zhen, S. R. Long, M. C. Wu, H. H. Shin, Q. Zheng, N.C. Yen, C. C. Tung, and H. H. Liu, “The empirical mode decomposition and the Hilbert spectrum for

nonlinear and non-stationary time series analysis," Proceedings of the Royal Society of London, vol. 454, no. A, pp. 903-995, 1998.

[51] C. T. Chen, H. C. Chen, Y. Y. Hu, and C. C. Wong, " Fuzzy balancing control of a small-size humanoid robot based on accelerometer," International Journal of Fuzzy Systems, vol. 11, no. 3, pp. 146-153, Sep. 2009.

[52] C. T. Lin and C. S. G. Lee, Neural Fuzzy Systems, Prentice-Hall, 1999.

Publication List

Journal Papers

[1] H. J. Liu, and K. Y. Young, "An adaptive upper arm EMG-based robot control system," *International Journal of Fuzzy Systems*, vol. 12, no. 3, pp 181-189, Sep. 2010.

[2] H. J. Liu, and K. Y. Young, "An efficient approach for EMG-based robot control," *International Journal of Electrical Engineering*, vol. 17, no. 5, pp 327-336, Oct. 2010.

[3] H. J. Liu, and K. Y. Young, "Applying wave-variable-based sliding mode impedance control for robot teleoperation," Accepted by *International Journal of Robotics and Automation*.

[4] H. J. Liu, and K. Y. Young, "Upper limb EMG-based robot motion governing using empirical mode decomposition and adaptive neural fuzzy inference system," in preparation for submission to *Journal of Intelligent and Robotic Systems*.

Conference Papers

[1] H. J. Liu, and K. Y. Young, "Robot motion governing using upper limb EMG signal based on empirical mode decomposition," *IEEE Conference on Systems Man and Cybernetics*, pp. 441-446, Oct. 2010.

[2] H. J. Liu and K. Y. Young, "Dealing with a bilateral teleoperation system with varying

time delay," *National Symposium on System Science and Engineering*, Taipei, Taiwan, June, 2007.

[3] H. J. Liu, P. C. Liu, and K. Y. Young, "Robot motion governing based on forearm EMG signals," *International Conference on Service and Interactive Robotics*, Taipei, Taiwan, August, 2009.